



Paleoclimatic controls on mercury deposition in northeast Brazil since the Last Interglacial

Omotayo Anuoluwapo Fadina^a, Igor Martins Venancio^b, Andre Belem^c,
Carla Semiramis Silveira^a, Denise de Castro Bertagnolli^d, Emmanoel Vieira Silva-Filho^a,
Ana Luiza S. Albuquerque^{a,*}

^a Department of Geochemistry, Federal Fluminense University, Outeiro São João Baptista s/n. - Centro, Niterói, 24020-141, Brazil

^b Center for Weather Forecasting and Climate Studies (CPTEC), National Institute for Space Research (INPE), Cachoeira Paulista, Brazil

^c Oceanographic Observatory, Federal Fluminense University, Passo da Pátria, 156 block E room 300, Praia Vermelha Campus - São Domingos, Niterói, 24210-240, Brazil

^d Department of Chemistry, Federal Fluminense University, Rua Desembargador Hermídio Ellys Figueira, 783 Aterrado, Volta Redonda, RJ, 27.213-145, Brazil

ARTICLE INFO

Article history:

Received 22 April 2019

Received in revised form

5 August 2019

Accepted 6 August 2019

Available online xxx

Keywords:

Mercury variations

Marine sediments

Glacial/interglacial climate

Millennial-scale events

South American continental margin

Northeastern Brazil

ABSTRACT

The sediment core GL-1248, collected from the continental slope off northeastern Brazil, was used to reconstruct mercury (Hg) variations in NE South American continental margin and understand its variability in response to paleoclimate changes over the past 128 ka. Mercury concentrations in GL-1248 ranged between 14.95 and 69.43 ng/g, showing a glacial-interglacial pattern with higher (lower) concentrations in the glacial period (interglacial period). Parallel trends of Hg and XRF-Fe plots suggest that following atmospheric Hg deposition onto the continent, Hg is incorporated with Fe compounds before transportation and eventual immobilization at the NE Brazil continental slope. Peaks of Hg and Fe/Ca ratio peaks occurred concurrently during certain Heinrich Stadials, indicating that Hg is transported from the continent alongside fluvial sediments during periods of increased precipitation and erosion in NE Brazil continent. Mercury concentrations varied with periodicities of 56 ka and 900 yr suggesting glacial-interglacial changes and millennial-scale variability, respectively. Total Hg and total organic carbon are poorly correlated, although the latter likely influenced Hg sequestration into marine sediments during millennial-scale events between 60 ka and 30 ka. Altogether, our results suggest that the atmosphere is the primary source of Hg to GL-1248 and glacial-interglacial climate variations were the major determinant of atmospheric Hg deposition. Furthermore, increased precipitation during millennial-scale events played a secondary role by enhancing Hg transport to the continental slope of NE Brazil.

© 2019 Published by Elsevier Ltd.

1. Introduction

Mercury (Hg) is a globally distributed metal of environmental concern due to its toxicity to both wildlife and human health (WHO, 1989). It is released into the environment via natural (volcanoes, geothermal vents, and rock weathering) and anthropogenic (industrial activities, mining and coal burning) (Amos et al., 2013) sources during pre-industrial and industrial times respectively. Owing to its atmospheric residence time of up to 1.5 years (Nriagu

et al., 1992; Santos et al., 2001), Hg can be transported from its point sources to remote locations, as far as the Antarctic and Arctic (Schroeder and Munthe, 1998; Horowitz et al., 2014; Steffen et al., 2015). Its sources and post-depositional fluxes within all environments constitute the global Hg biogeochemical cycle. Irrespective of its source, Hg stored in environmental reservoirs can be emitted back into the atmosphere or remobilized to secondary locations. Although several studies describe Hg depositional and post-depositional processes, recent studies on Hg variations in environmental archives highlight the role of climate in modulating Hg deposition and accumulation.

Hg emissions from natural sources (mainly volcanic eruptions) into the atmosphere are the largest and an essential component of the global Hg cycle (Gworek et al., 2016), with concentrations in natural archives varying over past climatic cycles (Jitaru et al.,

* Corresponding author. LOOP - Laboratório Oceanografia Operacional e Paleoclimatologia, Departamento de Geoquímica, Universidade Federal Fluminense, Outeiro São João Baptista s/n. - Centro, Niterói, RJ, Brazil.

E-mail address: ana_albuquerque@id.uff.br (A.L.S. Albuquerque).

2009). Its dynamics in the environments are controlled by global and regional climatic factors such as productivity, sea ice cover, riverine discharge, sea level changes, and precipitation patterns. Studies of sedimentary Hg profiles in environmental archives such as lake sediments, peats, glacial ice, and marine sediments have been used in paleoclimatic and paleoenvironmental reconstructions (Nriagu et al., 1992; Engstrom and Swain, 1997; Santos et al., 2001) in order to understand how natural processes affect Hg cycling in the environment. For example, Vandal et al. (1993) and Jitaru et al. (2009) recorded higher Hg deposition during cold climates than in warm climates, thus highlighting the role of high atmospheric dust loads on Hg deposition during the former. In addition, several studies have identified organic matter (OM) as the major driver of Hg accumulation in ocean sediments, a finding supported by significant positive correlations between total organic carbon (TOC) and Hg variations in the respective archives (Grasby et al., 2013; Kita et al., 2013, 2016). To determine the effect of the Intertropical Convergence Zone (ITCZ) on atmospheric Hg deposition, Kuss et al. (2011) and Soerensen et al. (2014) both compared atmospheric and aquatic Hg concentrations across the latitudinal transect of the Atlantic Ocean (Kuss et al., 2011; Soerensen et al., 2014). Aquatic Hg concentrations were found to be higher in the surface water below the Intertropical Convergence Zone (ITCZ) compared to those of other latitudes, regardless of the low atmospheric Hg concentration near the ITCZ location. Therefore, the authors concluded that precipitation in the ITCZ favors Hg-wet deposition into the surface water below the ITCZ.

In terms of the effects of forest fires on Hg emission, although their impacts are evident only in specific instances (Corella et al., 2017), forest fires are significant in the release of mercury (Hg) stored in vegetation and soils into the atmosphere. Consequently, high frequency and intensity of forest fires will likely result in increased mercury emissions from soils (Amos et al., 2013). Mercury emissions from volcanic activity and forest fires have been registered in mountain lakes from the Northern Patagonian Andes (Daga et al., 2016). In a study by Power et al. (2008), charcoal data suggested that the recorded rise in atmospheric Hg concentration is consequent to an increase in fire activity during the Last Glacial Maximum at the tropical latitudes of South America. Similarly, according to Cordeiro et al. (2011), warmer temperatures and the high rates of forest fires of the late Holocene in the Brazilian Amazon are key factors which lead to increased mercury deposition. Although several studies (e.g. Martínez Cortizas et al., 1999; Jitaru et al., 2009; Outridge et al., 2007; Kirk et al., 2011), have established that Hg profiles are driven by climate-modulated processes, few studies in the southwestern Atlantic have addressed its glacial-interglacial variations. Santos et al. (2001) showed that the threefold increase in Hg deposition of a sediment core from Lake Pata (northern Amazon) during the Holocene compared with the Last Glacial Maximum (LGM) was due to the high temperatures and the prevalence of forest fires during the Holocene. Other studies also show that Hg fluxes were significantly higher during wet climate episodes compared to dry ones (Lacerda et al., 1999; Barbosa et al., 2004). In a recent study from Caço Lake, NE Brazil (Lacerda et al., 2017), Hg fluxes for the last 22 ka were associated with global changes in atmospheric dust and climate, as well as global volcanism. A large number of published studies (e.g. Outridge et al., 2007; Stern et al., 2009; Grasby et al., 2013, Kita et al., 2013, 2016) have established significant positive correlations between Hg and organic matter in environmental archives. Notwithstanding, some authors (e.g. Roulet et al., 1998; Oliveira et al., 2001; Fadini and Jardim, 2001), have identified uncharacteristic trends in Hg post-depositional process within South American soils and sediments that links Hg variations to Iron (Fe)-oxyhydroxides rather than with organic matter (Roulet et al., 1998;

Oliveira et al., 2001; Fadini and Jardim, 2001). Till date, studies on Hg concentrations and fluxes over the changing climate in the southwestern Atlantic are relatively short-termed, with the oldest record terminating around 45 ka (Santos et al., 2001). As such, insights into the effects of abrupt regional climate changes on mercury deposition and accumulation over long timescales are lacking. This study seeks to examine if Hg records from the continental slope of NE Brazil are consequent global climate changes. Furthermore, the roles played by both global and regional climate oscillations on Hg delivery at the study site will be discussed.

Here, we present reconstructed Hg deposition and accumulation over the last 128 ka from a marine sediment core (GL-1248) collected from the equatorial Brazil margin off the continental shelf of NE Brazil. Alongside relevant geochemical proxies namely total organic carbon, stable isotopes ($\delta^{13}\text{C}_{\text{org}}$ and $\delta^{15}\text{N}_{\text{org}}$), and Fe/Ca ratios, we are able to understand the various climate mechanisms that control mercury atmospheric Hg deposition and post-depositional processes. We examine the impact of concurrent global and regional climate processes on Hg variations over the last glacial-interglacial cycle.

2. Material and methods

2.1. Regional setting and sediment core location

Marine sediment core GL-1248 (0°55.2'S, 43°24.1'W, 2264 m water depth, 19.29 m long) was collected by Petrobras from the continental slope off northeastern Brazil, a location under the influence of the North Brazil Current (NBC) and at a distance of about 280 km to the north of the mouth of the Parnaíba River (Fig. 1). Located northwest to the core site at a distance of approximately 739 km is the mouth of Amazon River. The 6400 km long Amazon River is the world's largest river in terms of discharge volume (209,000 m³/s), and accounts for approximately a fifth of global freshwater discharge (Richey et al., 1990; Moura et al., 2016). Comparing the average distances of both rivers to the core site, the

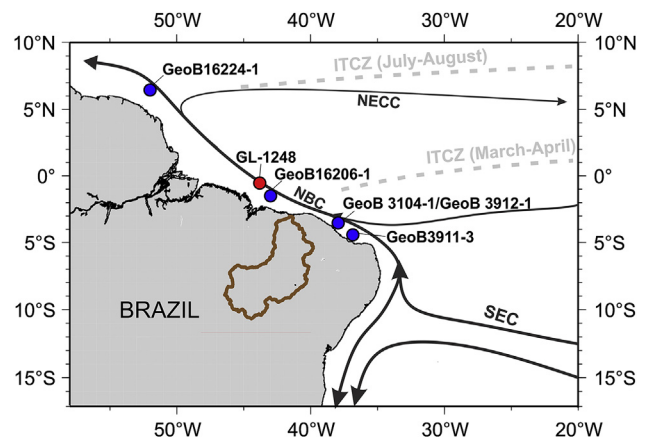


Fig. 1. Map of the study area showing the Parnaíba basin (Brown line), NE Brazil and the location of marine core GL-1248 (0°55.2'S, 43°24.1'W) in red dot. Blue dots represent other cores discussed in the text namely: GeoB 16206-1/1°34.75'S43°01.42'W and GeoB 16224-1/6°39.38'N52°04.99'W (Zhang et al., 2015) and GeoB 3104-1/GeoB 3912-1 (3°40.0'S, 37°43.0'W) and GeoB 3911-3/4°36.8'S, 36°38.2'W (Jennerjahn et al., 2004). The gray dotted lines show the seasonal positions of the Intertropical Convergence Zone (ITCZ) during boreal winter (July–August) and boreal summer (March–April) when it attains northernmost and southernmost positions respectively. Also shown are relevant surface currents namely the South Equatorial Current (SEC), the North Brazil Current (NBC) and North Equatorial Counter Current (NECC) in Black solid lines with arrows (adapted from Stramma and England, 1999). (For interpretation of the references to colour in this figure legend, the reader is referred to the Web version of this article.)

Parnaíba River is in closer proximity and as such more likely source of fluvial waters and terrestrial sediments to our core site. Its main course has a length of approximately 1400 km (Ramos et al., 2014), while the modern Parnaíba drainage basin area is approximately 344,000 km² (Marques et al., 2004). The Parnaíba River serves as a transition zone between the Caatinga's semi-arid land in the east area of the basin, and the more humid climate of Cerrado, in the west (Rosa et al., 2003; Ramos et al., 2014). The Caatinga is a mixed biome comprising of shrubs with areas of periodically dry forest (Leal et al., 2005), while the Cerrado is characterised by varying vegetation structure ranging from dense grassland with sparse shrubs coverings and small trees, to densely covered woodlands (Ratter et al., 1997). Dominant soil types in the basin include latosols, plinthosols, podzols, lithic soils and quartz sands (Paula Filho et al., 2015). The dominant vegetations in the region are the Caatinga, the Cerrado, the semideciduous forest and the coastal vegetation. Two transitional areas namely the Caatinga/Cerrado and Cerrado/Semideciduous forest have also been identified (Farias Castro, 2003).

The climate in northeastern Brazil is tropical and semi-humid with the raining season between the months of March through May. The precipitation regime is mainly influenced by seasonal Intertropical Convergence Zone (ITCZ) migrations (Hastenrath, 2012). In the boreal summer and fall when southeast (SE) trade winds are intense, the ITCZ is displaced northwards (Hastenrath and Merle, 1987). During boreal winter and spring when the northeast (NE) trade winds are intensified, the ITCZ attains its southernmost position, leading to enhanced precipitation in the Parnaíba River catchment (Hastenrath, 2012).

The upper water column circulation off northeast Brazil is mainly influenced by the NBC dynamics (Fig. 1). The NBC originates from the northern branch of the bifurcation of the South Equatorial Current (SEC) at 10°S (Stramma et al., 1995). The NBC transports warm and salty waters to the North Atlantic and the strength of its transport varies seasonally with the trade wind system. With an intensification of the SE trade wind during the boreal summer, the NBC flows north eastwards retroflecting at 6°–7°N (Johns et al., 1998) and feeding the North Equatorial Counter Current (NECC) which transports surface waters eastwards (Richardson and Reverdin, 1987). Conversely, when the NE trade winds gain strength during boreal winter, NBC transport reduces (Stramma et al., 1995; Johns et al., 1998) leading to the weakening or total absence of NECC thereby aiding NBC north-westward flow along the South American continental margin (Hastenrath and Merle, 1987; Stramma et al., 1995).

2.2. Sediment core chronology

Chronology of core GL-1248 was fully described by Venancio et al. (2018). The age model is based on 12 Accelerator Mass Spectrometry (AMS) radiocarbon ages on 400–500 planktonic foraminifera (*Globigerinoides ruber* and *Trilobatus sacculifer*) tests, which were handpicked from the fraction larger than 150 µm for the upper 6.30 m of the core. The radiocarbon dating reached 43.674 ka at 6.30 m depth. The chronology of the lower part of the core (6.30 - to 16.66 m core depth; ≈ 44–129 ka), was obtained by aligning the Ti/Ca record of core GL-1248 to the ice δ¹⁸O record of the North Greenland Ice Core Project (NGRIP) (NGRIP Members, 2004) using the extended Greenland Ice Core Chronology (GICC05modelext). According to Venancio et al. (2018), the alignment is based on the assumption that Greenland stadials are associated with increased precipitation over northeastern Brazil and increased delivery of terrigenous material to the western equatorial Atlantic, as supported by speleothem and marine records of the last glacial period (Jaeschke et al., 2007; Wang et al.,

2004; Zhang et al., 2015). The main Ti/Ca fluctuations of core GL-1248 were matched with corresponding major changes in δ¹⁸O from the NGRIP record, with tie points being mostly located at the midpoint of abrupt excursions on both records. Also, the start of the Last Interglacial was defined by aligning the Ti/Ca record of core GL-1248 with the Antarctic methane record from EPICA Dome C (Loulergue et al., 2008) at approximately 129 ka on the AICC2012 timescale (Veres et al., 2013), similar to previous studies (Govin et al., 2012). The basis for this tuning is that abrupt Greenland warming events occurred simultaneously with methane increases during millennial-scale events of the last glacial period and the last deglaciation (Baumgartner et al., 2014; Chappellaz et al., 1993; Huber et al., 2006). Radiocarbon ages and tie points defined for GL-1248 with their respective 2σ errors are summarized in Supplementary Table 1.

2.3. Geochemical analysis

Core GL-1248 was sampled every 5 cm (323 samples) for bulk analysis. Samples were decarbonated before total organic carbon (TOC), and stable isotopes (δ¹³C and δ¹⁵N) analyses. Each sample was encapsulated in tin (Sn) foil after carbonate removal by acidification with 1 M HCl, 60 mg of dried and pulverized sediment. The bulk analysis was performed using a PDZ Europa ANCA-GSL elemental analyzer at the Stable Isotope Facility of the University of California, Davis (USA) within an analytical precision of ±0.09%.

Elemental intensities of core GL-1248 were obtained by scanning the split core surfaces of the archive halves with X-ray fluorescence (XRF) Core-Scanner II (AVAATECH Serial No. 2) at the MARUM, University of Bremen (Germany). The XRF data were measured downcore every 0.5 cm in the core by irradiating a surface of about 10 mm × 12 mm for 20 s at 10 kV (Venancio et al., 2018).

For the determination of total Hg concentrations, 2 g of sediment was freeze-dried and lyophilized using TERRONE® lyophilizer for 24 h. Following homogenization, about 30 mg of each sample was analyzed using Zeeman Mercury Spectrometer RA-915 + according to the procedure described by Sholupov et al. (2004). Total Hg analysis was carried out at 5 cm interval and in triplicates for quality control, with Relative Standard Deviation (RSD) of ≤5% as the acceptable level of precision. The analytical method was further validated through the analysis of the certified reference material (PACS-2) purchased from the National Research Council Canada (NRCC). A total of 10 replicates were analyzed, having a recovery of 100% for elemental mercury. The detection limit was 0.5 ng/g for 10–400 mg of sediment. Analysis for total Hg concentrations was carried out at the Department of Geochemistry, Federal Fluminense University, Niteroi, Brazil.

Iron (Fe) oxy-hydroxides were extracted using the citrate-dithionate-bicarbonate (cdb) buffer method as described by Lucotte and d'Anglejan, (1985), and then analyzed by Inductively Coupled Plasma Atomic Emission Spectroscopy (ICP-AES) on a Shimadzu, model ICPE-9000. Quality control was assessed by analysis of blank reagents and using six (6) samples prepared in duplicate and analyzed at random positions within a batch and the analytical precision of these measurements is better than ±8%.

2.4. Mineralogical analysis

Mineralogical characterization was carried out on pulverized representative samples from two (2) depths within each marine oxygen isotope stage (MIS), using a Bruker D8 Advance X-ray powder diffractometer (XRD) with Cu Kα radiation at the Institute of Physics, Federal Fluminense University, Niteroi, Brazil. Diffractograms were collected using 2θ between 3° to 70° with a step-

size of 0.02° and 1.0s scanning time. For mineral identification, generated patterns were compared with tables from Brindley and Brown (1980) and data from the Mineralogy Database (<http://webmineral.com/>), similar to the methodology adopted by Silveira et al. (2016).

2.5. Time series analysis

In order to verify the presence of periodicities in our data, a spectral analysis on GL-1248 Hg results using the REDFIT algorithm (Schulz and Mudelsee, 2002) of the PAST software package (Hammer et al., 2001) was performed. For this analysis, a setting of two segments tapered with a Welch spectral window was selected, the oversampling factor was set to 4. Subsequently, the primary data set of Hg, in addition to other indicators such as TOC (discrete samples) and Fe/Ca ratio (XRF), and secondary data from other sources were analyzed using cross wavelet-spectral and cross-coherence techniques (Grinsted et al., 2004). Wavelets are two-dimensional transformations that present information about the distribution of events with relative energy to the whole time series, isolating the scale (frequency) of individual events (Grinsted et al., 2004; Salmond, 2005). The cross-wavelet is a bivariate version of the spectral analysis for comparing two sets of data (eg, Davis, 2002). Torrence and Webster (1999) and Grinsted et al. (2004) provide detailed explanations of the cross-wavelet, in particular the coherence and the cross-phase angle using the Morlet wavelet based on a continuous wavelet transform. In this technique, Monte Carlo simulations are used to provide a distribution of frequency-specific probability (global spectrum of wavelets) that can be tested by wavelet coefficients. Although discrete Hg data of this study and other paleo-proxies are not regularly spaced in time (along the core), Prokoph and El Bilali (2008) have shown that uncertainty in geological time scales due to stratigraphic error which adds non-stationary to paleoclimatic records can be minimized with a good interpolation process. In this work, the data of Hg, TOC, Fe/Ca and other paleo-proxies were interpolated with a resolution of 50 yr, using the nearest neighbors' interpolation technique, which preserves all the original features of discrete data.

3. Results

3.1. Age model and sedimentation rates

The age model for the upper 6.3 m core depth of GL-1248 based on 12 AMS radiocarbon ages terminated at about 44.0 ± 0.7 ka. The alignment of Ti/Ca ratio from the XRF data of the lower part of the core (6.3–16.65 m) with $\delta^{18}\text{O}$ record from NGRIP extended till 128.7 ka. As described by Venancio et al. (2018) sedimentation rates (SR) from core GL-1248 exhibit large fluctuations. Within Marine Oxygen Isotope Stage (MIS) 5 (5a, 5b, 5c and 5d), SR vary considerably with the highest average SR occurring in MIS5a (25.7 cm/ka). Although the glacial period started with low SR in MIS 4 (mean = 13 cm/ka), it increased significantly in MIS 3 to an average value of 32.1 cm/ka. While the SR in MIS 5e are relatively constant with an average of 6.93 cm/ka, SR in MIS 1 are irregular and have a higher average of 16.28 cm/ka. At the interval 2.18 m–1.7 m core depth, unusually low SR (3 cm/ka) for the region and period (see Zhang et al., 2015) were recorded. An implication of this is the possibility of the presence of a hiatus. Although no significant lithological changes were observed, SR and other data are not reported for this interval (MIS 2; 1.7 m–2.18 m core depth; \approx 14–29 ka).

3.2. Total organic carbon (TOC), carbon/nitrogen ratio (C:N), $\delta^{13}\text{C}$ and $\delta^{15}\text{N}$

The result obtained from the bulk analyses shows the variation of TOC, C/N, $\delta^{13}\text{C}_{\text{org}}$, and $\delta^{15}\text{N}_{\text{org}}$ in GL-1248 since the Last Interglacial period (Fig. 2). Two major periods can be identified from the TOC concentrations which ranged from 0.42% to 1.22%, increasing and decreasing in glacial periods (as well as cold sub-stages of MIS 5) and interglacial periods (and warm sub-stages of MIS 5) respectively. C/N ratios follow the same glacial-interglacial pattern shown by TOC concentrations, displaying values between 4.5 and 12.75. $\delta^{13}\text{C}_{\text{org}}$ fluctuated throughout the studied periods between -24.21 per mil (‰) and -19.16 per mil (‰) although the values were fairly constant within MIS 3 around -21.74 ‰. $\delta^{15}\text{N}_{\text{org}}$ (org) followed a similar pattern ranging between 4.48 per mil (‰) and 7.52 per mil (‰) with an average of 5.91 per mil (‰).

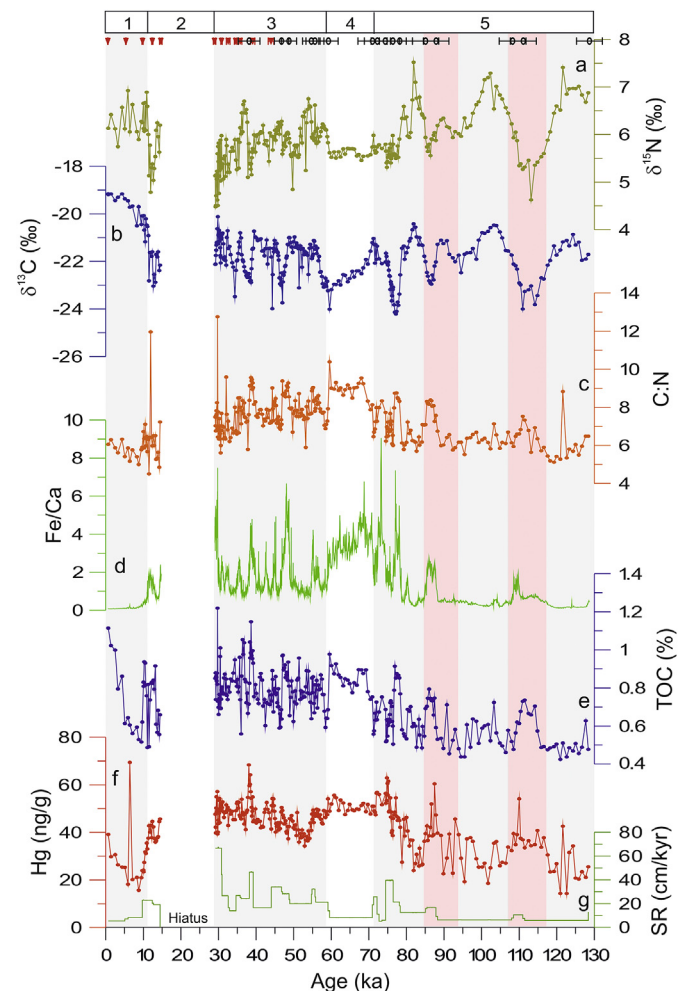


Fig. 2. Hg variation and paleoenvironmental proxies of the core GL-1248. (a) $\delta^{15}\text{N}_{\text{org}}$ in ‰ (olive green line) (b) $\delta^{13}\text{C}_{\text{org}}$ in ‰ (navy blue line) (c) Carbon-Nitrogen ratio (orange line) (d) Fe/Ca ratios (green line) (e) Total organic carbon (TOC) in % (blue line) (f) Total Hg concentration (red line) reported in ng/g (g) Sedimentation Rates (SR) in cm/kyr (green line). MIS boundaries in the studied time interval are numbered from 1 to 5. The red symbols represent calibrated radiocarbon dates while the open circles (black) are tie points with their respective 2σ error bars. (For interpretation of the references to colour in this figure legend, the reader is referred to the Web version of this article.)

3.3. Major element composition and Fe-oxyhydroxide (Fe_{cdb}) profile

The Fe/Ca ratios of core GL-1248 (Fig. 2d) show a clear trend of high values with frequent peaks in the glacial period and low values in the interglacial periods. A remarkable observation is the interruption of the baseline trend of Fe/Ca in MIS 5 by peaks, which occurred in MIS 5d and 5b. Peaks in the Fe/Ca ratios during MIS 4 and MIS 3 are coincident with millennial-scale events (Fig. 7).

Fe_{cdb} concentrations in our sediment core ranged from 0.01 to 0.45% and follow the Hg profile of higher concentrations in the cold periods of MIS 4 and 3 than during the interglacial periods (Fig. 5b). Also, higher Fe_{cdb} percentages occurred in the cold substages of MIS 5 (5d and 5b), similar with the mercury concentrations.

3.4. Hg concentrations

Mercury (Hg) concentrations in the sediment core ranged from 14.29 ng/g to 69.43 ng/g (average = 42.67 ng/g) having the highest concentration occurring at 6.4 ka within the current interglacial period (Fig. 2f). Sedimentary Hg concentrations were particularly high in glacial phases (MIS 4 and MIS 3), as well as in MIS 5d and 5b (MIS 5 cold sub-stages). In comparison, low concentrations were recorded in interglacial sediments and MIS 5 warm stages (MIS 5c and 5a).

3.5. Mineralogy

The mineralogical spectrum of all representative samples ($n = 16$) of core GL-1248 revealed a moderately varied array of minerals during the last 128 ka. The identified minerals in the marine sediment include kaolinite, goethite, feldspars, calcite, aragonite, quartz and halite (Supplementary Fig. 4). From the powder x-ray diffraction mineral identification of all samples, an alteration between continent and marine sourced minerals during glacial period (and cold substages) and interglacial periods (and warm substages) respectively was observed (Supplementary Table 1).

3.6. Time series analysis

When the discrete wavelet analysis is applied to the time series of Hg and TOC (Fig. 3), the millennial-scale signals can be identified throughout the series with greater intensity (5% significance level against red noise), especially during MIS 3 and MIS 5. Although with a lower significance, signals with longer periods in orbital scale (>23 k) presented strong spectral energy throughout the series time span.

Spectral analysis on the Hg concentrations from core GL-1248 revealed two significant periodicities (Fig. 4). The first one is centered at 56 ka and the second one at 900 yr. Both are significant over a 99% confidence level.

4. Discussion

4.1. Primary source of sedimentary mercury in marine sediment core GL-1248

Sedimentation rates of marine sediment core GL-1248 vary significantly over the studied period with high sedimentation rates up to 67.42 cm/ka during MIS 3 and lower sedimentation rates with averages of 16.28 cm/ka and 14.87 cm/ka during MIS 1 and MIS 5 respectively. Considering the proximity of our core to the adjoining continent and its location offshore Parnaíba River mouth (Fig. 1), marine sediments arriving and accumulating at the site are likely predominantly controlled by continental input from the Parnaíba

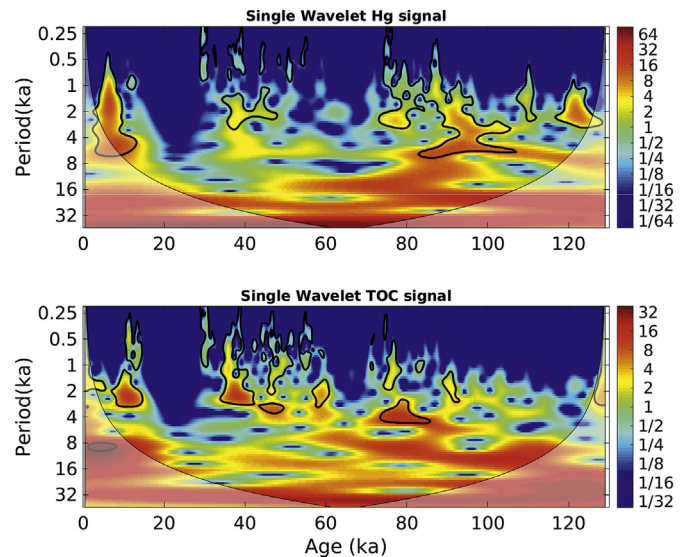


Fig. 3. The continuous wavelet power spectrum of Hg signal (top) and TOC (bottom). The thick black contour designates the 5% significance level against red noise and the Cone of Influence (COI) where edge effects might distort the picture is shown as a lighter shade. The wavelet show significant millennial periodicities in both TOC and Hg records. (For interpretation of the references to colour in this figure legend, the reader is referred to the Web version of this article.)

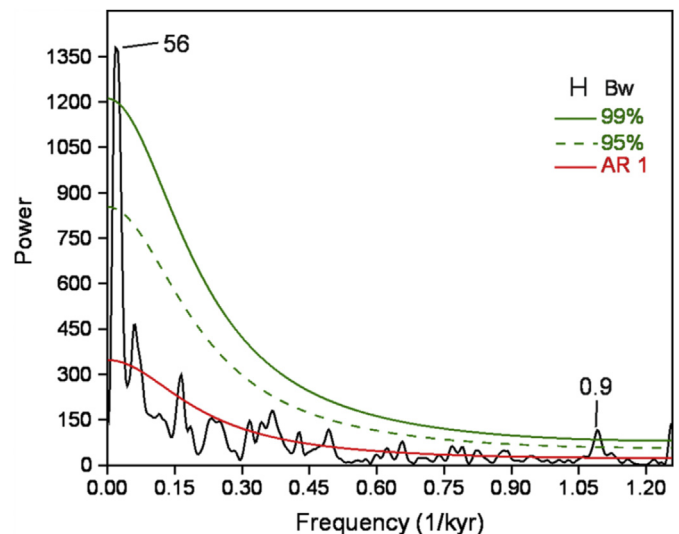


Fig. 4. Time series analysis performed with REDFIT (Schulz and Mudelsee, 2002) on GL-1248 Hg concentrations. The two periodicities that exceed the 95% (dashed green line) or 99% (solid green line) are labeled. The AR (1) red noise model (solid red line) and the bandwidth (black line; upper right corner) are displayed. (For interpretation of the references to colour in this figure legend, the reader is referred to the Web version of this article.)

Basin which are conveyed to the study site by fluvial transport. This conjecture is supported by the findings from a study by Lacerda et al. (2013) which showed that the distribution of metals (Al, Ba, Cu, Fe, Mn, Ni and Zn) in outer shelf sediments in NE Brazil at the Potiguar Basin are controlled by continental inputs from the proximal continent. In another study on the source of terrigenous materials to the NE South American continental margin, Zhang et al. (2015) showed, using neodymium (Nd) isotopic compositions of marine sediment cores GeoB16224-1 and GeoB16206-1, that terrigenous sediments deposited off NE Brazil, nearby our

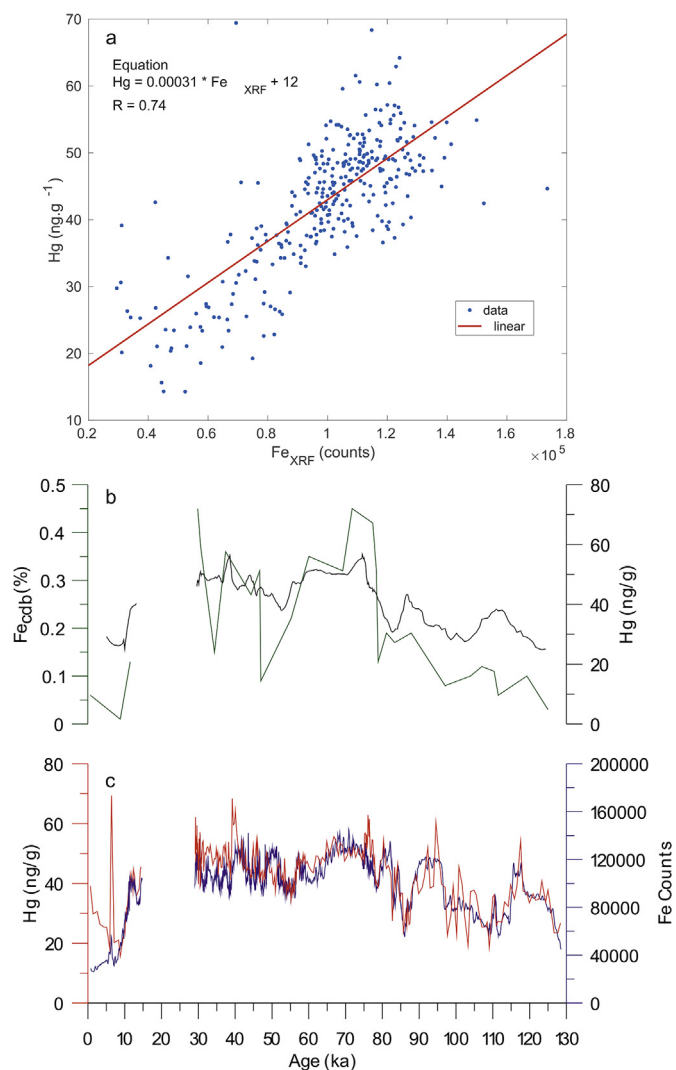


Fig. 5. Fe-Hg relationship across the studied period shown by: (a) linear regression between Fe counts (XRF) and Hg indicated by the trendline (red line), equation correlation coefficient ($R^2 = 0.74$). (b) Profile of Hg concentration (running averages shown in black line) and Fe_{cdB} in GL-1248 (green line). (c) Plot of Hg concentration in ng/g (red line) and running average of Fe counts (blue line). (For interpretation of the references to colour in this figure legend, the reader is referred to the Web version of this article.)

core location (Fig. 1), are not affected by Amazonian source. This latter finding is crucial to this study as it eliminates the Amazon as a potential source of Hg to GL-1248 since it has been established that the Amazon soils are a major link in the global Hg biogeochemical cycle due to their capacity to trap approximately 21% of global atmospheric Hg (Fostier et al., 2015). Thus, mercury in marine sediment core GL-1248 originates from the input of fluvial sediments transported by the Parnaíba River from the Parnaíba Basin offshore.

Mercury concentrations recorded in marine sediment GL-1248 (range = 14.29–69.43 ng/g; average 42.67 ng/g) over the last 128 ka are relatively lower than pre-industrial concentrations from Madeira River, southwest Amazonia (50–280 ng/g) [Lacerda et al., 1987], and Tapajós River, one of the major tributaries of the Amazon (10–140 ng/g) [Padberg, 1990]. In the southeastern part of Brazil, the Paraíba do Sul River, Pfeiffer et al. (1989) presented values between 300 and 550 ng/g. Although the reported Hg concentrations are quite dissimilar across respective locations, they are comparable considering that the concentrations were recorded

where no Hg-bearing geology exists (Wasserman et al., 2003; Lacerda et al., 2017), and date back to prehistoric times, therefore suggestive of the atmosphere as being a major source of the recorded Hg concentrations. Aula et al. (1994) measured Hg concentrations reaching 100 ng/g in the Tucuruí reservoir region, northern Brazil and concluded that the enrichment is a result of atmospheric Hg deposition. Similarly, Lacerda et al. (1999) using a record covering the last 30 ka from remote Amazonian lakes, which have no local Hg sources, attributed the Hg accumulation recorded to atmospheric inputs. In general, changes in Hg concentrations are linked to variations in atmospheric Hg sources or atmospheric conditions (Lacerda et al., 1999; Santos et al., 2001; Barbosa et al., 2004). These findings broadly support the outcome of a recent study from Caço Lake, NE Brazil (Lacerda et al., 2017), where the authors concluded that the atmosphere is the dominant source of Hg to the lake sediment. On account of the conclusion in these studies stating that the atmosphere is the major source of Hg to the South American continent, and the finding by Zhang et al. (2015) that Parnaíba Basin is the origin of terrigenous sediments deposited off NE Brazil, it is important to summarize the main post-depositional process related to Hg and the mineralogy of soils in Parnaíba Basin.

The Tropical soils of northeastern Brazil are notable for their high content of iron oxides mainly goethite and ferrihydrite; an amorphous Fe-oxyhydroxide precursor of hematite formation (Bigham et al., 2002). From the XRD result (Supplementary Table 2), goethite is present in all samples and we assume that other iron oxides (and oxyhydroxides) are also present but in uncrystallised amorphous state thus unidentifiable by the XRD. Fe-oxyhydroxides are important cementing agents and because of that, they play a pivotal role in metal adsorption processes in tropical soils (Selim, 2013). A positive correlation between deposited atmospheric Hg and Fe-oxyhydroxide (Fe_{cdB}) has been reported in tropical soil profiles (Roulet et al., 1998; Oliveira et al., 2001). This geochemical association of Hg with Fe_{cdB} in soils is supported by evidences of strong correlations between Fe_{cdB} and Hg profiles reported in soils and sediments originating from French Guiana (Roulet and Lucotte, 1995), Tapajós River (Roulet et al., 1996) and Rio Negro Basin (Fadini and Jardim, 2001). Other studies have also identified Fe-oxyhydroxides as an effective Hg-carrier phase (Laurier et al., 2003; Grimaldi et al., 2015) either by complexation with goethite (Forbes et al., 1974) or adsorption (Kinniburgh and Jackson, 1978; Schuster, 1991). In Fig. 5c, the profile of Fe counts covary with Hg concentrations in core GL-1248, and have a correlation coefficient of 0.74 ($p < 0.01$) (Fig. 5a) thereby suggesting that the Fe minerals in the sediment are significantly important in the accumulation of Hg in marine sediment GL-1248. Furthermore, the similar variations of Hg and its carrier-phase, Fe_{cdB} (Fig. 5b), suggest that iron oxyhydroxides are the principal factor controlling Hg profile in GL-1248. Although grain size distribution in sediments significantly influences trace/heavy metal concentration (Lim et al., 2017), Hg concentration in GL-1248 is poorly correlated ($R^2 = 0.024$) with both its clay and silt contents. The cross wavelet transform (Supplementary Fig. 1) show that Fe and Hg are in phase throughout the record, thus reinforcing that Fe-compounds in the marine sediment primarily determine the Hg variations. Altogether the described Hg-Fe (and Fe_{cdB}) relationships suggest that Hg in GL-1248 is transported alongside fluvial terrigenous sediments from NE Brazil continent to the core site. The Hg-bearing Fe_{cdB} particles are eroded from the Parnaíba Basin and transported by Parnaíba River until they are immobilized in the continental slope. The strong positive correlation between Hg and Fe-oxyhydroxides corroborates the outcome of aforementioned studies (Roulet and Lucotte, 1995; Roulet et al., 1996; Fadini and Jardim, 2001) that link Hg variations with Fe_{cdB} profiles in tropical soils. A similar

significant finding is that the peak of Hg concentration occurred concomitantly with Fe signal during the Mid-Holocene (Supplementary Fig. 5). This observed peak may be linked to the findings of Cruz et al. (2009), who reported using $\delta^{18}\text{O}$ ratios in cave speleothems from NE Brazil that significantly wetter conditions persisted during the Mid-Holocene, similar with paleoclimatic records from the north of NE Brazil (Montade et al., 2015) that attributed the development of rainforest in the region to the reduction of dry season between 17.5 ka and 15 ka. As such, the synchronous Hg-Fe peaks could be attributed to abrupt terrigenous material delivery, and it further confirms the association between Hg and Fe profiles in tropical soils, as well as the continental source of Hg records in GL-1248 sediments. However, the possible influence of fires on Hg concentration during the Holocene cannot be ruled out. Although the link between high Hg deposition and high frequency of forest fires in the Holocene has been raised by Santos et al. (2001), other authors have described the fire regime of the Holocene as unstable (Carcaillet et al., 2002; Cordeiro et al. 2008). In the study by Cordeiro et al. (2008), the authors recorded highest accumulation rates of charcoal particles, an indicator of paleo-fires, during the driest period of the Holocene, i.e., early and Mid - Holocene. Owing to the divergence in the findings of Cordeiro et al. (2008) from Eastern Amazon and Cruz et al. (2009) from NE Brazil, both suggesting dry and wet conditions respectively in the Mid-Holocene, the influence of forest fires on our Holocene Hg concentration needs to be interpreted with caution. However, it could be argued that the discrepancy is due to the site locations. Also, unlike other studies which explicitly discuss forest fires using high-resolution Holocene records, this study presents a lower resolution for the Holocene that is relatively fragmentary to allow definite conclusions.

4.2. Glacial-interglacial controls on Hg concentrations

As shown in Fig. 6, high Hg records during glacial periods are coincident with elevated dust deposition recorded in both Greenland (Ruth et al., 2007) and Antarctica (Lambert et al., 2008) ice cores. The similarity in dust plots from the two extreme locations supports the notion that high atmospheric dust loads are characteristic of glacial periods. Elevated Hg concentrations in the cold substages of MIS 5 (i.e. MIS 5d and 5b) are also concurrent with minor increases in dust concentrations above their minimum concentrations in the same substages (Fig. 6). Another possible dust source that can impact Hg deposition in glacial-interglacial timescales at our site is the Saharan dust (Kumar et al., 2014; Williams et al., 2006). We compared the Hg concentrations of core GL-1248 with dust fluxes from core MD03-2705 located on the coast of Africa (Skonieczny et al., 2019) and observed a good match between both datasets (Supplementary Fig. 2). Saharan dust fluxes increase during MIS4 and cold substages of MIS5, similar to our Hg concentrations from the western equatorial Atlantic. This gives further support to the influence of atmospheric dust concentrations on Hg deposition at our site. On a global scale, cold and dry climatic stages have been identified as periods with high dust levels that enhance rapid Hg sequestration from the atmosphere (Cordeiro et al., 2011). Jitaru et al. (2009) showed that Hg deposition in surface snows over the last 670 ka was notably higher during cold climates, as a consequence of high atmospheric dust loads. In a study by Vandal et al. (1993), the triple increase in Hg concentration in Dome C core from Antarctica between 27 and 17 ka, compared to both older and younger periods in the same record, was attributed to increased oceanic productivity. Comparing the findings of Vandal et al. (1993) with the core GL-1248, although both Hg and TOC concentration plots in this study exhibit similar variations by of higher records in glacial periods compared to interglacial periods, it

is important to note that the total organic carbon include incursions of terrestrial organic carbon to the study site. Despite the former being mainly of marine origin, the influx of terrestrial organic matter has the capacity to dilute marine organic matter (Machado et al., 2016). Consequently, Hg and TOC concentrations are poorly normalized and have a correlation coefficient of 0.18 (Supplementary Figs. 3a and 3b), thus implying that TOC is unlikely a major driver of Hg records in GL-1248. This finding is contrary to previous studies that have suggested a strong positive relationship between Hg and organic matter in sediments (Vandal et al., 1993; Outridge et al., 2007; Stern et al., 2009; Grasby et al., 2013; Kita et al., 2013, 2016), due to the fact that organic matter scavenges Hg within the water column through sorption, and subsequently deposits it in marine sediments (Hermanns et al., 2012). The outcome is however consistent with results on Hg-OM relationships from sites located in NE South America, where authors observed better correlations between Hg and iron (Fe) minerals rather than with organic matter (Roulet and Lucotte, 1995; Marins et al., 1998; Roulet et al., 1998; Wasserman et al., 2003; Selim, 2013). Therefore, it can be conceivably hypothesized that increasing (and decreasing) trends in Hg concentrations over glacial (and interglacial) periods in GL-1248 are in response to the changes in atmospheric Hg deposition onto the NE Brazil continent, which is controlled by the global variation in atmospheric dust loads. Likewise, the non-correlation between Hg and TOC in the marine sediments and existence of strong correlation and parallel trends of Hg and Fe concentration plots (Fig. 5) confirm the geochemical association reported by several authors which suggest that Fe compounds act as the carrier-phase of atmospheric Hg deposited onto tropical soils.

In previous studies of marine sediment cores collected in the coast of NE Brazil, Fe/Ca ratios was used as a proxy for terrigenous vs. marine input (Arz et al., 1998; Jaeschke et al., 2007; Govin et al., 2012). Higher Fe/Ca ratios are recorded during periods of increased terrigenous sediment influx relative to carbonate fraction. In these studies, elevated Fe/Ca values were reported within glacial periods due to low sea level and/or to increases in precipitation (wet phases). The occurrence of wet phases in NE Brazil during the glacial periods MIS 4 and MIS 3, when the mean SST reached 23.89 ± 0.79 °C, has been associated with Heinrich Stadials (Jennerjahn et al., 2004; Nace et al., 2014; Zhang et al., 2015). Further to the increase in terrigenous sediment delivery ensuing from enhanced precipitation, the latter also favours atmospheric Hg 'wet' deposition. Additionally, SST data from prior studies suggest that the glacial periods experienced the most SST reduction (Bard et al., 2000; Martrat et al., 2007). In like manner, notable SST reductions in the North Atlantic during the cold sub-stages MIS 5b and 5d are coincident with the extension of the Scandinavian ice sheets (Svendsen et al., 2004). During these periods of low SST and ice sheets enlargement, the relative sea-level is characteristically low. Therefore, the river mouth is nearer the core site, and the erosion of shelf sediments as well as enhanced deposition onto the continental slope (Lacerda et al., 2013; Nace et al., 2014) enhances the delivery of terrigenous materials to the core site. As shown in Fig. 6, during MIS 4 and MIS 3 when the RSL was significantly low with averages reaching -71.51 m and -69.03 m respectively, we observe high Fe/Ca values suggesting increased incursion of terrigenous materials offshore via Parnaíba River. This accords the findings of previous studies, which suggest enhanced delivery of terrigenous materials onto the continental slope of western South Atlantic during the glacial periods. Contrarily, the near baseline Fe/Ca ratios recorded in the interglacial periods signify lower terrestrial material delivery. Although both MIS 1 and 5e are interglacial periods, previous studies have suggested that the MIS 5e (SST = 28.9 °C) interglacial experienced higher temperatures than

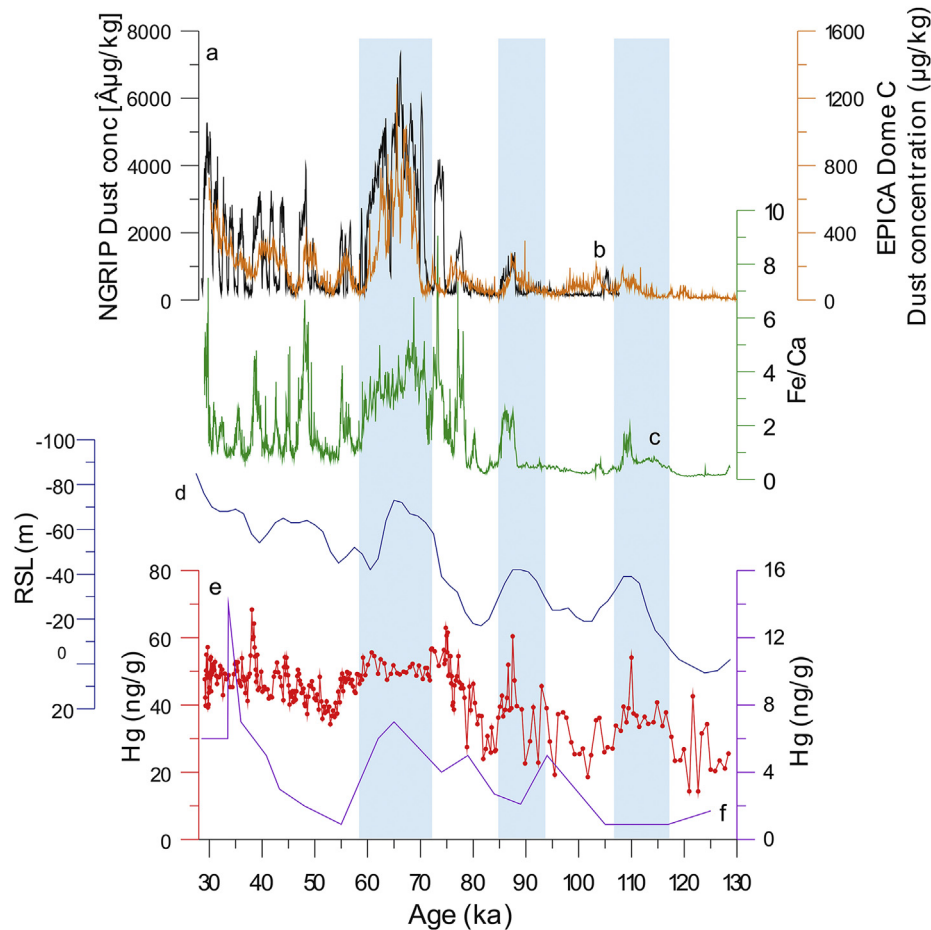


Fig. 6. (a) NGRIP ice core record of atmospheric dust deposition (Ruth et al., 2007) in black line (b) EPICA Dome C ice core record of atmospheric dust deposition (Lambert et al., 2008) in orange line (c) Fe/Ca ratio from GL-1248 indicating periods of high and low terrigenous sediment delivery to the study site in green line (d) Relative sea level (m) from Waelbroeck et al. (2002) in blue line. (e) Hg concentration in GL-1248 in red line. (f) Hg data from Antarctica (Jitaru et al., 2009) in purple line. High Hg dust concentrations, low sea levels and high amount of terrestrial load delivery to the core site are coincident with elevated Hg records in MIS 4 and 3 as well as in the cold substages of MIS 5 (5d and 5b). These cold periods are highlighted in blue bars. (For interpretation of the references to colour in this figure legend, the reader is referred to the Web version of this article.)

MIS 1 (SST = 28.3 C) (Rama-Corredor et al., 2015). This difference in SST between both interglacial periods has been attributed to precessional modulation (Martrat et al., 2014). As a result of the higher SST during MIS 5e, ice sheet reduction ensued and the global sea-level rose by up to 5 m than the modern sea-level (Hodgson et al., 2006; Rohling et al., 2007). The sea-level rise presumably positioned the core site farthest from the river mouth, thus reducing the amount of continental material and Hg delivery. Accordingly, it is significant to mention that the least average Hg concentration in this study was recorded in MIS 5e.

Carbon and nitrogen isotopic ratios ($\delta^{13}\text{C}_{\text{org}}$ and $\delta^{15}\text{N}_{\text{org}}$) of organic matter are proxies whose variability helps to understand the source and quality of organic matter in sediments. $\delta^{13}\text{C}_{\text{org}}$ distinguishes between marine and continental sedimentary organic matter, while $\delta^{15}\text{N}_{\text{org}}$ variations signify the changes in OM source and quality, with elevated values denoting high degrees of organic matter degradation during times of normal sedimentation, and vice versa (Meyers, 1994; Jennerjahn et al., 2004). The high variability of $\delta^{13}\text{C}_{\text{org}}$ values (fluctuating between -20‰ and -24‰) recorded in the glacial period (Fig. 2b) reflects changes in the origin of organic matter between marine and terrestrial sources. Jennerjahn et al. (2004) studied sedimentary cores from the continental margin of NE Brazil and observed decreases in $\delta^{13}\text{C}_{\text{org}}$ from -20‰ to values between -23‰ and -24‰ . The authors attributed the 3‰

reduction to a contribution of terrestrial organic matter to the study site. Seeing that our $\delta^{13}\text{C}_{\text{org}}$ values vary similarly with theirs considering the proximity of the sediments cores in their study to this present study (Fig. 1), we can infer that the $\delta^{13}\text{C}_{\text{org}}$ variation indicates the influx (as a result of low sea-level as explained in the previous paragraph) of terrestrial organic matter mainly produced by C3 land plants. Supporting the findings of Jennerjahn et al. (2004) in the same study who ascribed minimum (maximum) $\delta^{15}\text{N}_{\text{org}}$ values to low (high) sedimentation rates in NE Brazil continental shelf, Zhang et al. (2015) have showed that in the glacial periods when the sea level was low, most of the NE Brazilian shelf was exposed and rapid sedimentation of river-transported terrestrial material on the continental slope occurred. The findings suggest that the minimum $\delta^{15}\text{N}_{\text{org}}$ values (average 5.8‰) recorded in the glacial periods can be attributed to high sedimentation rates ensuing from increased continental runoff, whereas maximum $\delta^{15}\text{N}_{\text{org}}$ values occurred in the interglacial periods (average 6.05‰) depicting average sedimentation conditions. Altogether, the $\delta^{13}\text{C}_{\text{org}}$ and $\delta^{15}\text{N}_{\text{org}}$ variations in GL-1248 support the earlier hypothesis that higher amounts of continent-derived materials were deposited on the continental slope of NE Brazil in the glacial periods as opposed to interglacial periods. These results are consistent with our XRD mineralogy results which follow the same glacial-interglacial alteration in the origin marine sediment GL-1248

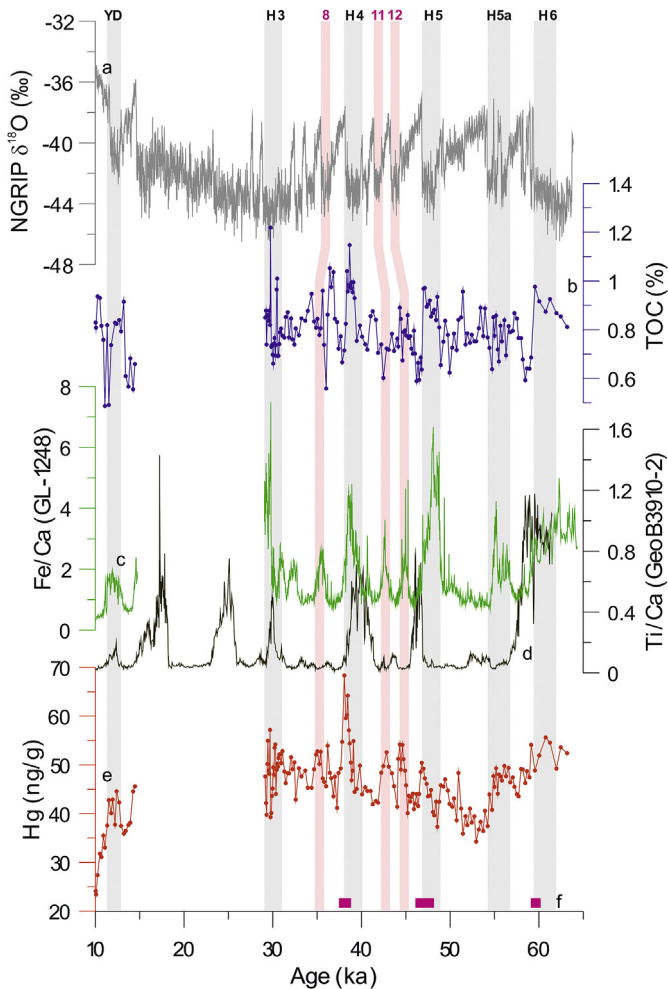


Fig. 7. Millennial-scale (MS) variability as shown by the comparison of Hg and Fe/Ca ratio from GL-1248 with NGRIP data and other proxies from NE Brazil. (a) Speleothem growth phases (pink rectangles) consequent to increased precipitation in NE Brazil (Wang et al., 2004). (b) Hg record (orange line) from core GL-1248. (c) Fe/Ca (green line) from core GL-1248 (d) Ti/Ca record from core GeoB3910-2 (black line) collected off northeastern Brazil (Jaeschke et al., 2007) (e). TOC from GL-1248 (purple line). (f) $\delta^{18}\text{O}_{\text{ice}}$ from NGRIP on the GICC05 model time scale (gray line). Heinrich Stadials (HS 6-3) and Younger Dryas (YD) are marked in gray bars. The pink coloured bars mark the Dansgaard-Oeschger stadials 8, 11 and 12 respectively. (For interpretation of the references to colour in this figure legend, the reader is referred to the Web version of this article.)

from a continental source during glacial period (and cold substages) to a marine source during interglacial periods (and warm substages) [Supplementary Table 1].

In general, Hg concentration in core GL-1248 varied in response to glacial-interglacial changes. To further support this, time series analysis of Hg concentration (Fig. 4) show a peak centered in 56 ka (half eccentricity) indicating glacial-interglacial variability. The elevated Hg concentrations recorded in glacial periods are favored by a combination of global (high atmospheric dust loads) and regional (augmented wet deposition, precipitation, enhanced erosion, and material transport and low sea level) climatic factors. In contrast to glacial periods, the interglacial periods (MIS 1 and MIS 5e) and the warm sub stage of MIS 5 (MIS 5c) witnessed opposing climatic conditions. Since interglacial periods present less atmospheric dust deposition (Jitaru et al., 2009) and high sea-level, as well as low regional precipitation and nominal erosion, the outcome of this contrasting climatic trend in the warm periods is the lower Hg concentrations recorded in the core (Fig. 9 a and b).

However, inconsistent with these trends during interglacial periods and warm substage MIS 5c, Hg peaks occurred at the end of MIS 5a. These peaks are coincident with Fe/Ca peaks and they correlate with Dansgaard-Oeschger (DO) stadials.

4.3. Millennial-scale events recorded by Hg concentrations

Several marine sediment cores collected offshore northeastern Brazil show Fe/Ca and Ti/Ca peaks during Heinrich Stadials (HS) (Arz et al., 1998; Jaeschke et al., 2007; Nace et al., 2014). Wang et al. (2004) also observed speleothem growth phases, correlating with HS1, HS5, and HS6, as a result of increased precipitation, at 10°S in northeastern Brazil. Similarly, large pulses of terrigenous sediment supply offshore NE Brazil, indicative of wet phases, have been observed during the Younger Dryas (YD) (Jaeschke et al., 2007; Deplazes et al., 2013; Nace et al., 2014; Zhang et al., 2015), although Bouimetarhan et al. (2018) identified two distinct and dissimilar wet conditions during the YD. In addition to the evidences on HS and YD signals in the tropics, Dansgaard-Oeschger (DO) variability has been recorded in sediments of the Cariaco Basin (Deplazes et al., 2013) and NE Brazil (Venancio et al., 2018). Enhanced precipitation over northeastern Brazil during DO stadials coincide with dry periods in Cariaco Basin (Jaeschke et al., 2007), thus signifying an anti-phase response in precipitation patterns between both locations. Likewise, in a study by Wang et al. (2006), the authors observed that the millennia-scale variations in the oxygen isotopic record of speleothems from southern Brazil are anti-correlated with records from eastern China. This anti-phase pattern in both records was attributed to the seasonal north-south shift in the mean position of the ITCZ. Tropical signals of millennial-scale variability which ensued from north Atlantic cold events are associated with the reductions in AMOC strength, and the accompanying southward ITCZ migration that prompted wetter conditions and continental runoff in NE Brazil (Broccoli et al., 2006; Stouffer et al., 2006; Montade et al., 2015; Mulitza et al., 2017). As a consequence of increased precipitation, palynological records from NE Brazil have shown tropical rainforest expansion during the wet period of the YD (Bouimetarhan et al., 2018) and during HS1 (Montade et al., 2015). It is also noteworthy that during HS precipitation patterns have changed in eastern South America not only due to a southward displacement of the ITCZ, but also because of an intensification of the South American Monsoon System (SAMS) as showed recently by Strikis et al. (2018).

Consistent with these studies, abrupt increases in the Fe/Ca ratios from core GL-1248 (Fig. 7d) are observed during certain millennial-scale events. In addition, certain Hg peaks occur within these periods and coincide with these Fe/Ca peaks of millennial-scale events. Specifically, distinct rises in Hg concentrations which are synchronous with Fe/Ca peaks are observed in Heinrich Stadials 5a, HS5, HS4 and the Younger Dryas, as well as DO-12, 11 and 8 (Fig. 7). The observation of elevated Hg concentrations during millennial-scale events is consistent with findings from numerous studies which show that millennial climate change are strongly correlated with active Quaternary volcanism (Bay et al., 2004; Baldini et al., 2015), thus, it is anticipated that the atmosphere is burdened with more Hg from volcanic eruptions during these millennial-scale events. In like manner, the possible influence of Sahara dust on GL-1248 sediment, and by extension its Hg concentrations, cannot be ruled out owing to the fact that Prospero et al. (1981) showed that high quantities of dusts are transported from the Sahara Desert to mainly South America. Combining the findings of Moreno et al. (2002) which showed that Saharan wind intensity increased during D-O and the Heinrich Stadials, with the observation of high Hg concentrations during HS4 and the YD in core GL-1248 which are synchronous to increases in Saharan dust

flux (Supplementary Fig. 2), it is possible that Saharan dust may play a role in Hg deposition at our site during millennial-scale events. Correspondingly, Hg fluctuates with periods of 900 yr (Fig. 4), thus reinforcing the evidence of millennial-scale variability in our Hg records. However, different from glacial-interglacial variations where sea level change was a major determinant of Hg variations, changes in Hg concentration during stadials were not influenced by sea level fluctuations since sea level changes are not significant in the millennial timescale. In Fig. 8, we show a comparison of original Hg concentrations with the same Hg data but extracting the effect of sea level variation. It is observed that although millennial frequencies are present in both graphs, their statistical power increases after filtering the sea level change. This confirms the masking effect of sea level fluctuations on the millennial-scale variability in our record.

The observed rise in our Hg record during millennial climate variability could be explained by a sequence of climate mechanisms which ensue from the southward positioning of the ITCZ during the stadials (Broccoli et al., 2006; Stouffer et al., 2006). Noting that high frequency of volcanism in this period will increase the background levels of atmospheric Hg, increased precipitation during millennial-scale events will boost atmospheric Hg deposition on the continent (wet deposition). Furthermore, influx of fluvial sediments by the Parnaíba River created by intensified fluvial erosion on the Parnaíba Basin will contribute to the increased transportation and deposition of terrigenous materials at the continental slope of NE Brazil during these millennial-scale events (Fig. 9c). While it could be argued that direct atmospheric Hg deposition over the ocean is equally a noteworthy contribution to our sedimentary Hg records, the observed Fe-Hg correlation described in sub-sections 4.1 and 4.2 suggests that Hg in GL-1248 is essentially from a continental (secondary) source. It is important to note that despite the evidences of millennial-scale variability in Hg records of GL-1248 sediment core, discrepancies in the magnitudes of both Hg and Fe/Ca peaks are evident during these events (Fig. 7d and f). For

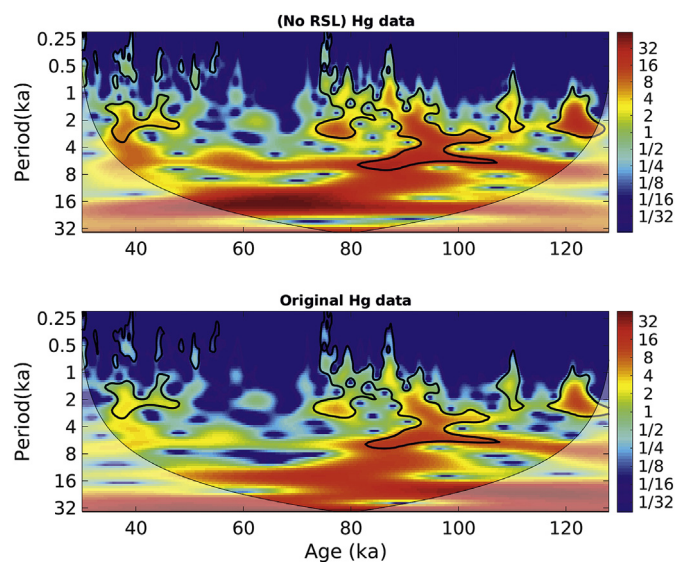


Fig. 8. The continuous wavelet power spectrum of Hg signal without relative sea level (RSL) influence (upper panel) and original Hg signal (lower panel). The thick black contour designates the 5% significance level against red noise and the cone of influence (COI) where edge effects might distort the picture is shown as lighter shade. The upper panel show an increase in statistical power (color scale) in periodicities related to millennial-scale variability (periods in ka are marked in the left y-axis) after the removal of RSL influence, which shows the masking effect of RSL changes on the millennial-scale variability in our Hg record. (For interpretation of the references to colour in this figure legend, the reader is referred to the Web version of this article.)

example, the Fe/Ca peaks are well-defined in HS5a to HS3 (Fig. 7d), whereas only HS4 is distinct in Hg records (Fig. 7f). Following the idea that Hg is transported alongside eroded continental material from NE Brazil via the Parnaíba River to the core site, in the absence of other mechanisms controlling Hg variation in sediments, the amount of Hg delivered at the study site should be consistent with continental material delivery as indicated by the Fe/Ca ratios. Thus, both records should present a similar trend in the magnitude of their peaks. With the lack of this expected comparable trend, it could be argued that the observed millennial-scale events in our Hg record are unlikely to be solely related to precipitation and erosion intensification, due to ITCZ southward displacement. Surprisingly, enhanced organic matter deposition shown by increasing TOC values occurred during millennial-scale events with their amplitudes varying similarly with those of Hg (Fig. 7b). In the cross wavelet transform of TOC and Hg time series (Supplementary Fig. 1), an in-phase relationship between the two parameters evident by right pointing arrows occasionally between 90 ka and 60 ka in the 6 ka band. Furthermore, arrows between periods 30 ka and 75 ka point upwards and indicate a dominance of TOC over Hg. The implication of this is that both TOC and Hg show some correlation at the mentioned intervals. These observed changes in total organic carbon concentrations during millennial-scale events are in line with earlier findings (Jennerjahn et al., 2004; Sachs and Anderson, 2005; Menviel et al., 2008). Since TOC variations influence Hg sequestration into marine sediments, it is possible that the sedimentary Hg records during these periods are somewhat inclusive of the sequestration of “free” Hg (unbound to Fe-compounds) by the total organic carbon in the water column, followed by immobilization in marine sediment, a finding that is supported by various studies (Outridge et al., 2007; Stern et al., 2009; Grasby et al., 2013; Kita et al., 2013, 2016). Hence, it can be hypothesized that, although TOC is not a major driver of sedimentary Hg variations throughout the studied period in marine sediment GL-1248, the likelihood of its influence in certain periods cannot be dismissed. This is further supported by the fact that the correlation coefficient (R^2) generated from the plots of TOC and Hg is not 0 (i.e. $R^2 \neq 0$), rather they are poorly correlated ($R^2 = 0.18$) (Supplementary Fig. 3b). These findings suggest that Hg variations in GL-1248 during millennial-scale events are modulated by changes in fluvial transport and slightly influenced by TOC.

5. Conclusions

Mercury concentrations in GL-1248 collected from the continental slope off northeastern Brazil varied over the last glacial-interglacial cycle. The atmosphere is the main source of Hg accumulation in the western South Atlantic. Fe-oxyhydroxides, a major component of tropical Brazil soils, was the major carrier-phase of Hg in the soils, during transportation until immobilization at our core site, although total organic carbon might have aided Hg sedimentation during millennial-scale events (Fig. 9). Changes in global atmospheric dust concentrations and climate over the studied timescale contributed significantly to atmospheric Hg deposition in Parnaíba basin. Mercury records show that atmospheric Hg deposition was higher in the glacial periods than in interglacial periods (Conceptual models shown in Fig. 9a and b). Regional factors such as precipitation pattern, runoff events and sea level changes control Hg remobilization from the continent to its secondary location, the study site. Peaks of Hg are correlated with peaks of Fe/Ca ratios from NE Brazil confirming that Hg delivered at our site was transported with fluvial materials during continental runoff events corresponding to millennial-scale variability (Fig. 9c). We showed that (1) the atmosphere is the primary source of our sedimentary Hg records and factors such as volcanism, variation in

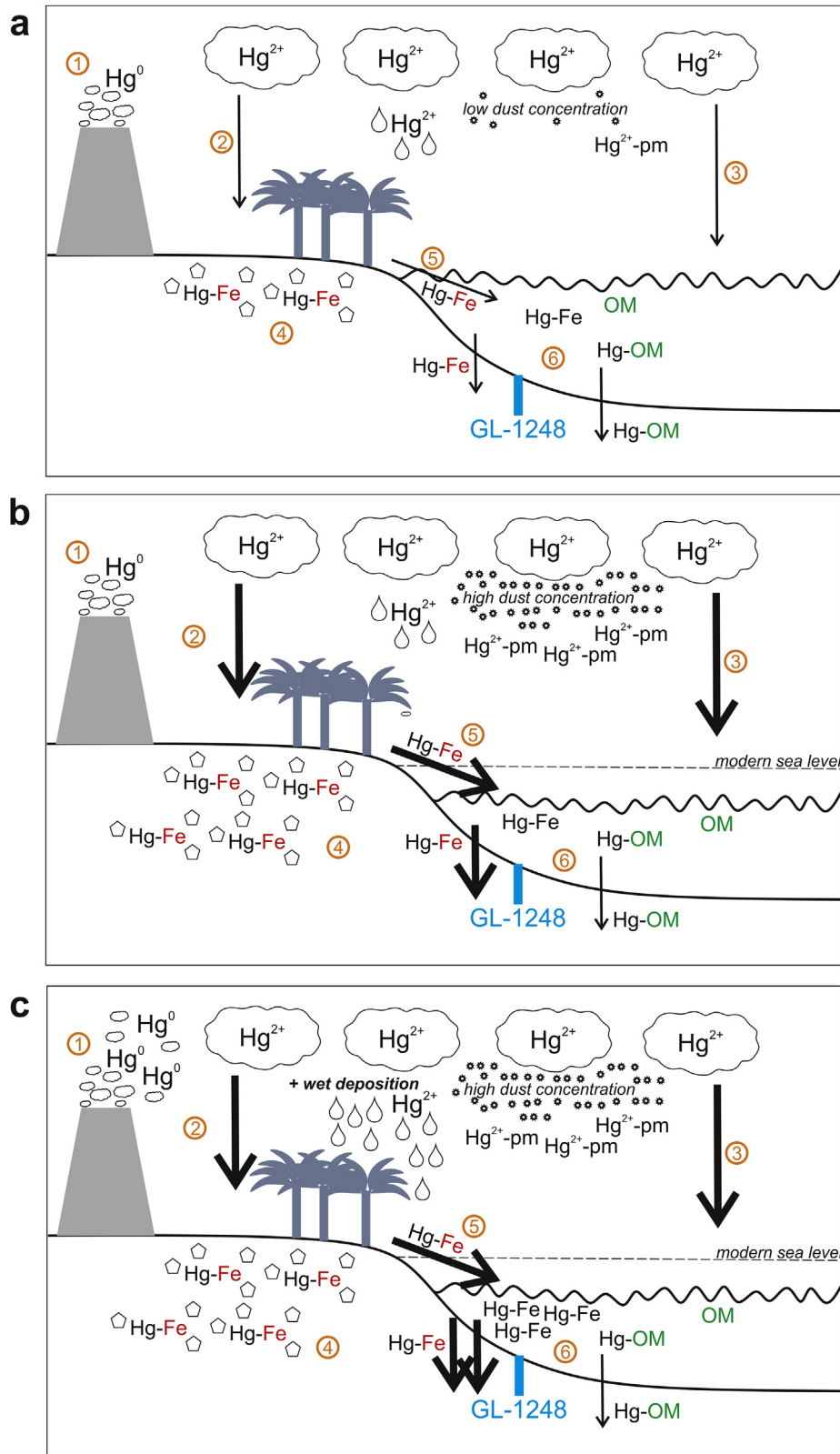


Fig. 9. Conceptual model showing the processes controlling mercury deposition and accumulation in the study area. ① Volcanic emission ② Deposition (continent) ③ Deposition (ocean) ④ Complexation with Fe-minerals ⑤ Runoff/erosion ⑥ Immobilization/sedimentation. (a) Modern condition. During the interglacial period when atmospheric dust load concentration is low, minimal atmospheric Hg is deposited onto the NE Brazil continent. (b) Glacial condition. The glacial period is characterised by high atmospheric dust loads, as such, high amounts of Hg is deposited onto the NE Brazil continent. Consequent to the variations in amounts of Hg being deposited from the atmosphere to the continent in 9a and 9b, more Hg-bearing terrigenous materials were immobilized in the continental slope in the glacial period compared to the interglacial period. (c) Millennial-scale stadal conditions. Intensified precipitation during millennial-scale events complemented atmospheric Hg deposition by wet deposition. Enhanced erosion in the NE Brazil continent during these events contributed to the increased transport and deposition of terrigenous materials to the continental slope.

atmospheric dust concentrations, sea-level changes and precipitation patterns influence its deposition as well as transportation, and (2) due to Hg post-depositional processes and remobilization, Parnaíba Basin served as the secondary source of Hg reaching the marine sediment core location. The findings of this study suggest that Hg delivered at the continental slope off northeastern Brazil is consequent to both global and regional climate phenomena, the latter being millennial-scale variability and superimposed by the former (glacial-interglacial variations).

Acknowledgment

We are grateful for funding from CAPES-ASPECTO project (grant 88887.091731/2014-01) and PALEOCEANO-CAPES (23038.001417/2014-71). A.L.S. Albuquerque is a CNPq (National Council for the Development of Science and Technology, Brazil) senior researcher (grant 302521/2017-8). We profoundly thank R. Kowsman (CENPES/Petrobras) and Petrobras Core Repository staff (Macaé/Petrobras) for supplying the sediment used in this study. CAPES currently financially support Igor M. Venancio with a scholarship (Grant 88887.156152/2017-00 and 88881.161151/2017-01). This study was financed in part by the Coordenação de Aperfeiçoamento de Pessoal de Nível Superior - Brasil (CAPES) - Finance Code 001.

Appendix A. Supplementary data

Supplementary data to this article can be found online at <https://doi.org/10.1016/j.quascirev.2019.105869>.

References

- Amos, H.M., Jacob, D.J., Streets, D.G., Sunderland, M., 2013. Legacy impacts of all-time anthropogenic emissions on the global mercury cycle. *Glob. Biogeochem. Cycles* 27, 410–421. <https://doi.org/10.1002/gbc.20040>.
- Arz, H.W., Pätzold, J., Wefer, G., 1998. Correlated millennial-scale changes in surface hydrography and terrigenous sediment yield inferred from Last-Glacial marine deposits off northeastern Brazil. *Quat. Res.* 50 (2), 157–166. <http://doi.org/10.1006/qres.1998.1992>.
- Aula, I., Braunschweiler, H., Leino, T., Malin, I., Porvari, P., Hatanaka, T., Lodenius, M., Juras, A., 1994. Levels of mercury in the Tucuruí reservoir and its surrounding area in Pará, Brazil. In: Watras, C.J., Huckabee, J.W. (Eds.), *Mercury Pollution: Integration and Synthesis*. Lewis Publishers, Boca Raton, pp. 21–40.
- Baldini, J.U.L., Brown, R.J., McElwaine, J.N., 2015. Was millennial-scale climate change during the Last Glacial triggered by explosive volcanism? *Sci. Rep.* 5, 17442. <https://doi.org/10.1038/srep17442>.
- Barbosa, J.A., Cordeiro, R.C., Silva, E.V., Turcq, B., Gomes, P.R.S., Santos, G.M., Sifeddine, A., Albuquerque, A.L.S., Lacerda, L.D., Hausladen, P.A., Tims, S.G., Levchenko, V.A., Fifield, L.K., 2004. 14C-MAS as a tool for the investigation of mercury deposition at a remote Amazon location. *Nucl. Instrum. Methods Phys. Res. B* 223/224, 528–534.
- Bard, E., Rostek, F., Turon, J.L., Gendreau, S., 2000. Hydrological impact of Heinrich events in the subtropical northeast Atlantic. *Science* 289, 1321–1324.
- Baumgartner, M., Kindler, P., Eicher, O., Floch, G., Schilt, A., Schwander, J., et al., 2014. NGRIP CH₄ concentration from 120 to 10 kyr before present and its relation to a $\delta^{15}N$ temperature reconstruction from the same ice core. *Clim. Past* 10 (2), 903–920. <http://doi.org/10.5194/cp-10-903-2014>.
- Bay, R.C., Bramall, N., Price, P.B., 2004. Bipolar correlation of volcanism with millennial climate change. *Proc. Natl. Acad. Sci. U. S. A.* 101 (17), 6341–6345. <https://doi.org/10.1073/pnas.0400323101>.
- Bigham, J.M., Fitzpatrick, R.W., Schulze, D., 2002. Iron oxides. In: Dixon, J.B., Schulze, D.G. (Eds.), *Soil Mineralogy with Environmental Applications*. Soil Science Society of America Book Series, Madison, pp. 323–366.
- Bouimetarhan, I., Chiessi, C.M., González-Arango, C., Dupont, L., Voigt, I., Prange, M., Zonneveld, K., 2018. Intermittent development of forest corridors in northeastern Brazil during the last deglaciation: climatic and ecologic evidence. *Quat. Sci. Rev.* 192, 86–96. <https://doi.org/10.1016/j.quascirev.2018.05.026>.
- Brindley, G.W., Brown, G. (Eds.), 1980. *Crystal Structures of Clay Minerals and Their X-Ray Identification*. Mineralogical Society of Great Britain and Ireland, p. 518.
- Broccoli, A.J., Dahl, K.A., Stouffer, R.J., 2006. Response of the ITCZ to northern hemisphere cooling. *Geophys. Res. Lett.* 33 (1). <http://doi.org/10.1029/2005GL024546>.
- Carcaillet, C., Almquist, H., Asnong, H., Bradshaw, R.H.W., Carrion, J.S., Gaillard, M.-J., Gajewski, K., Haas, J.N., Haberle, S.G., Hadorn, S.P., Müller, D., Richard, P.J.H., Richoiz, I., Rosch, M., Sanchez Goni, M.F.S., von Stedingk, H., Stevenson, A.C., Talon, B., Tardy, C., Tinner, W., Tryterud, E., Wick, L., Willis, K.J., 2002. Holocene biomass burning and global dynamics of the carbon cycle. *Chemosphere* 49, 845–863. [https://doi.org/10.1016/S0045-6535\(02\)00385-5](https://doi.org/10.1016/S0045-6535(02)00385-5).
- Chappellaz, J., Blunier, T., Raynaud, D., Barnola, J.M., Schwander, J., Stauffert, B., 1993. Synchronous changes in atmospheric CH₄ and Greenland climate between 40 and 8 kyr BP. *Nature* 366 (6454), 443–445. <http://doi.org/10.1038/366443a0>.
- Cordeiro, R., Turcq, B., Suguio, K., Oliveiradasilva, A., Sifeddine, A., Volkmerribeiro, C., 2008. Holocene fires in East Amazonia (Carajás), new evidences, chronology and relation with paleoclimate. *Glob. Planet. Chang.* 61 (1–2), 49–62. <https://doi.org/10.1016/j.gloplacha.2007.08.005>.
- Cordeiro, R.C., Turcq, B., Sifeddine, A., Lacerda, L.D., Silva Filho, E.V., Gueiros, B., Potty, Y.P., Santelli, R.E., Pádua, E.O., Pachinelam, S.R., 2011. Biogeochemical indicators of environmental changes from 50 ka to 10 ka in a humid region of the Brazilian Amazon. *Palaeogeogr. Palaeoclimatol. Palaeoecol.* 299, 426–436. <https://doi.org/10.1016/j.palaeo.2010.11.021>.
- Corella, J.P., Wang, F., Cuevas, C.A., 2017. 700 years reconstruction of mercury and lead atmospheric deposition in the Pyrenees (NE Spain). *Atmos. Environ.* 155, 97–107. <https://doi.org/10.1016/j.atmosenv.2017.02.018>.
- Cruz, F.W., Vuille, M., Burns, S.J., Wang, X., Cheng, H., Werner, M., Edwards, L.R., Karmann, I., Auler, A.S., Nguyen, H., 2009. Orbitally driven eastwest antiphasing of South American precipitation. *Nat. Geosci.* 2, 210–214. <https://doi.org/10.1038/ngeo444>.
- Daga, R., Ribeiro Guevara, S., Pavlin, M., Rizzo, A., Lojen, S., Vreča, P., Horvat, M., Arribère, M., 2016. Historical records of mercury in southern latitudes over 1600 years: lake Futalaufquen, northern Patagonia. *Sci. Total Environ.* 553, 541–550. <https://doi.org/10.1016/j.scitotenv.2016.02.114>.
- Davis, J.C., 2002. *Statistics and Data Analysis in Geology*, third ed. Wiley, New York.
- Deplazes, G., Lückge, A., Peterson, L.C., Timmermann, A., Hamann, Y., Hughen, K.A., Röhl, U., Laj, C., Cane, M.A., Sigman, D.M., Haug, G.H., 2013. Links between tropical rainfall and North Atlantic climate during the last glacial period. *Nat. Geosci.* 6, 1–5. <https://doi.org/10.1038/ngeo1712>.
- Engstrom, D.R., Swain, E.B., 1997. Recent declines in atmospheric mercury deposition in the upper Midwest. *Environ. Sci. Technol.* 31, 960–967. <http://doi.org/10.1021/es9600892>.
- Fadini, P.S., Jardim, W.F., 2001. Is the Negro river basin (Amazon) impacted by naturally occurring mercury? *Sci. Total Environ.* 275, 71–82. [https://doi.org/10.1016/S0048-9697\(00\)00855-X](https://doi.org/10.1016/S0048-9697(00)00855-X).
- Farias Castro, A.A.J., 2003. Survey of the vegetation in the state of Piauí. In: Gaiser, T., Krol, M., Frischkorn, H., de Araújo, J.C. (Eds.), *Global Change and Regional Impacts*. Springer, Berlin, Heidelberg, pp. 117–123. https://doi.org/10.1007/978-3-642-55659-3_9.
- Forbes, E.A., Posner, A.M., Quirk, J.P., 1974. The specific adsorption of inorganic Hg(II) species and Co(III) complex ions on goethite. *J. Colloid Interface Sci.* 49, 403–409. [https://doi.org/10.1016/0021-9797\(74\)90385-3](https://doi.org/10.1016/0021-9797(74)90385-3).
- Fostier, A.H., Melendez-Perez, J.J., Richter, L., 2015. Litter mercury deposition in the Amazonian rainforest. *Environ. Pollut.* 206, 605–610. <https://doi.org/10.1016/j.envpol.2015.08.010>.
- Govin, A., Holzwarth, U., Heslop, D., Ford Keeling, L., Zabel, M., Mulitza, S., Chiessi, C.M., 2012. Distribution of major elements in Atlantic surface sediments (36°N–49°S): imprint of terrigenous input and continental weathering. *Geochim. Geophys. Res.* 13 (1), 1525–2027. <https://doi.org/10.1029/2011gc003785>.
- Grasby, S.E., Sanei, H., Beauchamp, B., Chen, Z., 2013. Mercury deposition through the Permo-triassic Biotic crisis. *Chem. Geol.* 351, 209–216. <https://doi.org/10.1016/j.chemgeo.2013.05.022>.
- Grimaldi, M., Guédron, S., Grimaldi, C., 2015. Impact of gold mining on mercury contamination and soil degradation in Amazonian ecosystems of French Guiana. In: Brearley, F.Q., Thomas, A.D. (Eds.), *Land-use Change Impacts on Soil Processes: Tropical and Savannah Ecosystems*. CABI, Wallingford, UK, pp. 95–107.
- Grinsted, A., Moore, J.C., Jevrejeva, S., 2004. Application of the cross wavelet transform and wavelet coherence to geophysical time series. *Nonlinear Process Geophys.* 11, 561–566.
- Gworek, B., Bemowska-Kalabun, O., Kijeńska, M., Wrzosek- Jakubowska, J., 2016. Mercury in marine and oceanic waters - a review. *Water Air Soil Pollut.* 227 (10), 371. <https://doi.org/10.1007/s11270-016-3060-3>.
- Hammer, Ø., Harper, D.A. Ta.T., Ryan, P.D., 2001. PAST: Paleontological statistics software package for education and data analysis. *Palaeontol. Electron.* 4 (1), 1–9 (1). <http://doi.org/10.1016/j.bcp.2008.05.025>.
- Hastenrath, S., 2012. Exploring the climate problems of Brazil's Nordeste: a review. *Clim. Change.* <http://doi.org/10.1007/s10584-011-0227-1>.
- Hastenrath, S., Merle, J., 1987. Annual cycle of subsurface thermal structure in the tropical Atlantic Ocean. *J. Phys. Oceanogr.* 17 (9), 1518–1538. [https://doi.org/10.1175/1520-0485\(1987\)017%3c1518:ACOSTS%3e2.0.CO;2](https://doi.org/10.1175/1520-0485(1987)017%3c1518:ACOSTS%3e2.0.CO;2).
- Hermanns, Y.-M., Cortizas, A.M., Arz, H., Stein, R., Biester, H., 2012. Untangling the influence of in-lake productivity and terrestrial organic matter flux on 4,250 years of mercury accumulation in Lake Hambro, Southern Chile. *J. Paleolimnol.* 49, 563–573. <https://doi.org/10.1007/s10933-012-9657-7>.
- Horowitz, H.M., Jacob, D.J., Amos, H.M., Streets, D.G., Sunderland, E.M., 2014. Historical mercury releases from commercial products: global environmental implications. *Environ. Sci. Technol.* 48, 10242–10250. <https://doi.org/10.1021/es501337j>.
- Huber, C., Leutenberger, M., Spahni, R., Flückiger, J., Schwander, J., Stocker, T.F., et al., 2006. Isotope calibrated Greenland temperature record over marine isotope stage 3 and its relation to CH₄. *Earth Planet. Sci. Lett.* 243 (3–4), 504–519.

- <https://doi.org/10.1016/j.epsl.2006.01.002>.
- Hodgson, D.A., Verleyen, E., Squier, A.H., Sabbe, K., Keely, B.J., Saunders, K.M., Vyverman, W., 2006. Interglacial environments of coastal east Antarctica: comparison of MIS 1 (Holocene) and MIS 5e (Last Interglacial) lake-sediment records. *Quat. Sci. Rev.* 25 (1–2), 179–197. <https://doi.org/10.1016/j.quascirev.2005.03.004>.
- Jaeschke, A., Rühlemann, C., Arz, H., Heil, G., Lohmann, G., 2007. Coupling of millennial-scale changes in sea surface temperature and precipitation off northeastern Brazil with high-latitude climate shifts during the last glacial period. *Paleoceanography* 22 (4). <http://doi.org/10.1029/2006PA001391>.
- Jennerjahn, T.C., Venugopalan, I., Arz, H.W., Behling, H., Pätzold, J., Wefer, G., 2004. Asynchronous terrestrial and marine signals of climate change during Heinrich Events. *Science* 306, 2236–2239. <http://doi.org/10.1126/science.1102490>.
- Jitaru, P., Gabrielli, P., Marteel, A., Plane, J.M.C., Planchon, F.A.M., Gauchard, P.A., Ferrari, C.P., Boutron, C.F., Adams, F.C., Hong, S., Cescon, P., Barbante, C., 2009. Atmospheric depletion of mercury over Antarctica during glacial periods. *Nat. Geosci.* 2 (7), 505–508. <https://doi.org/10.1038/ngeo549>.
- Johns, W.E., Lee, T.N., Beardsley, R.C., Candela, J., Limeburner, R., Castro, B., 1998. Annual cycle and variability of the north Brazil current. *J. Phys. Oceanogr.* 28 (1), 103–128. [https://doi.org/10.1175/1520-0485\(1998\)028%3c0103:ACAVOT%3e2.0.CO;2](https://doi.org/10.1175/1520-0485(1998)028%3c0103:ACAVOT%3e2.0.CO;2).
- Kinniburgh, D.G., Jackson, M.L., 1978. Adsorption of mercury (II) by iron hydrous oxide gel. *Soil Sci. Soc. Am. J.* 42, 45–47. <https://doi.org/10.2136/sssaj1978.03615995004200010010x>.
- Kirk, J.L., Muir, D.C.M., Antoniadou, D., Douglas, M.S.V., Evans, M.S., Jackson, T.A., Kling, H., Amoureux, S., Lim, D.S.S., Pienitz, R., et al., 2011. Climate change and mercury accumulation in Canadian high and subarctic lakes. *Environ. Sci. Technol.* 45 (3), 964–970. <https://doi.org/10.1021/es102840u>.
- Kita, I., Kojima, M., Hasegawa, H., 2013. Mercury content as a new indicator of ocean stratification and primary productivity in Quaternary sediments off Bahama Bank in the Caribbean Sea. *Quat. Res.* 80, 606–613. <https://doi.org/10.1016/j.yqres.2013.08.006>.
- Kita, I., Yamashita, T., Chiyonobu, S., Hasegawa, H., Sato, T., Kuwahara, Y., 2016. Mercury content in Atlantic sediments as a new indicator of the enlargement and reduction of Northern Hemisphere ice sheets. *J. Quat. Sci.* 31 (3), 167–177. <https://doi.org/10.1002/jqs.2854>.
- Kuss, J., Züllicke, C., Pohl, C., Schneider, B., 2011. Atlantic mercury emission determined from continuous analysis of the elemental mercury sea-air concentration difference within transects between 50° N and 50° S. *Glob. Biogeochem. Cycles* 25, GB3021. <https://doi.org/10.1029/2010GB003998>.
- Kumar, A., Abouchami, W., Galer, S., Garrison, V., Williams, E., Andreae, M., 2014. A radiogenic isotope tracer study of transatlantic dust transport from Africa to the Caribbean. *Atmos. Environ.* 82, 130–143. <https://doi.org/10.1016/j.atmosenv.2013.10.021>.
- Lacerda, L.D., Turcq, Bruno, Sifeddine, Abdel, Cordeiro, Renato Campello, 2017. Mercury accumulation rates in Caço Lake, NE Brazil during the past 20,000 years. *J. South Am. Earth Sci.* (77), 42–50. <https://doi.org/10.1016/j.jsames.2017.04.008>.
- Lacerda, L.D., Campos, R.C., Santelli, R.E., 2013. Metals in water, sediments and biota of an offshore oil exploration area in the Potiguar Basin, northeastern Brazil. *Environ. Monit. Assess.* (185), 4427–4447. <http://doi.org/10.1007/s10661-012-2881-9>.
- Lacerda, L.D., Ribeiro, M.G., Cordeiro, R.C., Sifeddine, A., Turcq, B., 1999. Atmospheric mercury deposition over Brazil during the past 30,000 years. *Ciênc. Cultura J. Braz. Assoc. Adv. Sci.* 51, 363–371.
- Lacerda, L.D., Pfeiffer, W.C., Silveira, E.G., Bastos, W.R., Souza, C.M.M., 1987. Contaminação por mercúrio na Amazônia; análise preliminar do rio Madeira, RO. In: *Anais do II Congresso Brasileiro de Geoquímica. Sociedade Brasileira de Geoquímica, Rio de Janeiro, RJ*, pp. 295–299.
- Lambert, F., Delmonte, B., Petit, J.R., Bigler, M., Kaufmann, P.R., Hutterli, M.A., Stocker, T.F., Ruth, U., Steffensen, J.P., Maggi, V., 2008. Dust-climate couplings over the past 800,000 years from the EPICA Dome C ice core. *Nature* 452, 616–619. <https://doi.org/10.1038/nature06763>.
- Laurier, F.J.G., Cossa, D., Gonzalez, J.L., Breviere, E., Sarazin, G., 2003. Mercury transformations and exchanges in a high turbidity estuary: the role of organic matter and amorphous oxyhydroxides. *Geochem. Cosmochim. Acta* 67, 3329–3345. [https://doi.org/10.1016/S0016-7037\(03\)00081-4](https://doi.org/10.1016/S0016-7037(03)00081-4).
- Leal, I.R., Silva, J.M.C., Tabarelli, M., Lacher Jr., T.E., 2005. Changing the course of biodiversity conservation in the Caatinga of northeastern Brazil. *Conserv. Biol.* 19 (3), 701–706. <https://doi.org/10.1111/j.1523-1739.2005.00703.x>.
- Lim, D., Kim, J., Xu, Z., Jeong, K., Jung, H., 2017. New evidence for Kuroshio inflow and deepwater circulation in the Okinawa Trough, East China Sea: sedimentary mercury variations over the last 20 kyr. *Paleoceanography* 32 (6), 571–579. <https://doi.org/10.1002/2017pa003116>.
- Loulergue, L., Schilt, A., Spahni, R., Masson-Delmotte, V., Blunier, T., Lemieux, B., et al., 2008. Orbital and millennial-scale features of atmospheric CH₄ over the past 800,000 years. *Nature* 453 (7193), 383–386. <http://doi.org/10.1038/nature06950>.
- Lucotte, M., d'Anglejan, B., 1985. A comparison of several methods for the determination of iron hydroxides and associated orthophosphates in estuarine particulate matter. *Chem. Geol.* (48), 257–264. [https://doi.org/10.1016/0009-2541\(85\)90050-6](https://doi.org/10.1016/0009-2541(85)90050-6).
- Machado, W., Sanders, C.J., Santos, I.R., Sanders, L.M., Silva-Filho, E.V., Luiz-Silva, W., 2016. Mercury dilution by autochthonous organic matter in a fertilized mangrove wetland. *Environ. Pollut.* 213, 30–35. <https://doi.org/10.1016/j.envpol.2016.02.002>.
- Marins, R.V., Lacerda, L.D., Paraquetti, H.H.M., de Paiva, E.C., Villas Boas Bull, R.C., 1998. Geochemistry of mercury in sediments of a sub-tropical coastal Lagoon, sepetiba Bay, southeastern Brazil. *Environ. Contam. Technol.* 61, 57–64.
- Marques, M., da Costa, M.F., Mayorga, M.I. de O., Pinheiro, P.R.C., 2004. Water environments: anthropogenic Pressures and ecosystem changes in the Atlantic drainage basins of Brazil. *AMBIO A J. Hum. Environ.* 33 (1), 68–77. <https://doi.org/10.1579/0044-7447-33.1.68>.
- Martínez Cortizas, A., Pontevedra-Pombal, X., García-Rodeja, E., Nóvoa-Muñoz, J.C., Shoty, W., 1999. Mercury in a Spanish peat Bog: archive of climate change and atmospheric metal deposition. *Science* 284 (516), 939–942. <https://doi.org/10.1126/science.284.5416.939>.
- Martrat, B., Grimalt, J.O., Shackleton, N.J., De Abreu, L., Hutterli, M.A., Stocker, T.F., 2007. Four climate cycles of recurring deep and surface water destabilizations on the Iberian margin. *Science* 317, 502–507. <https://doi.org/10.1126/science.1139994>.
- Martrat, B., Jimenez-Amat, P., Zahn, R., Grimalt, J.O., 2014. Similarities and dissimilarities between the last two deglaciations and interglaciations in the North Atlantic region. *Quat. Sci. Rev.* 99, 122–134. <https://doi.org/10.1016/j.quascirev.2014.06.016>.
- Menviel, L., Timmermann, A., Mouchet, A., Timm, O., 2008. Meridional reorganizations of marine and terrestrial productivity during Heinrich events. *Paleoceanography* 23 (PA1203). <http://doi.org/10.1029/2007PA001445>.
- Meyers, P.A., 1994. Preservation of elemental and isotopic source identification of sedimentary organic matter. *Chem. Geol.* 114 (3–4), 289–302. [https://doi.org/10.1016/0009-2541\(94\)90059-0](https://doi.org/10.1016/0009-2541(94)90059-0).
- Montade, V., Kageyama, M., Combourieu-Nebout, N., Ledru, M.-P., Michel, E., Siani, G., Kissel, C., 2015. Teleconnection between the Intertropical Convergence Zone and southern westerly winds throughout the last deglaciation. *Geology* 43 (8), 735–738. <http://doi.org/10.1130/g36745.1>.
- Moreno, A., Cacho, I., Canals, M., Prins, M.A., Sánchez-Goni, M.-F., Grimalt, J.O., Weltje, G.J., 2002. Saharan dust transport and high-latitude glacial climatic variability: the Alboran sea record. *Quat. Res.* 58 (03), 318–328. <http://doi.org/10.1006/qres.2002.2383>.
- Moura, R.L., Amado-Filho, G.M., Moraes, F.C., Brasileiro, P.S., Salomon, P.S., Mahiques, M.M., et al., 2016. An extensive reef system at the Amazon River mouth. *Sci. Adv.* 2, 1501252. <http://doi.org/10.1126/sciadv.1501252>.
- Multiza, S., Chiessi, C.M., Schefuß, E., Lippold, J., Wichmann, D., Antz, B., Mackensen, A., Paul, A., Prange, M., Rehfeld, K., Werner, M., Bickert, T., Frank, N., Kuhnert, H., Lynch-Stieglitz, J., Portillo-Ramos, R.C., Sawakuchi, A.O., Schulz, M., Schwenk, T., Tiedemann, R., Vahlenkamp, M., Zhang, Y., 2017. Synchronous and proportional deglacial changes in Atlantic meridional overturning and north-east Brazilian precipitation. *Paleoceanography* 32 (6), 622–633. <http://doi.org/10.1002/2017PA003084>.
- Nace, T.E., Baker, P.A., Dwyer, G.S., Silva, C.G., Rigsby, C.A., Burns, S.J., Zhu, J., 2014. The role of North Brazil Current transport in the paleoclimate of the Brazilian Nordeste margin and paleoceanography of the western tropical Atlantic during the late Quaternary. *Palaeogeogr. Palaeoclimatol. Palaeoecol.* 415, 3–13. <http://doi.org/10.1016/j.palaeo.2014.05.030>.
- North Greenland Ice Core Project members, 2004. High-resolution record of Northern Hemisphere climate extending into the last interglacial period. *Nature* 431 (7005), 147–151. <http://doi.org/10.1038/nature02805>.
- Nriagu, J.O., Pfeiffer, W.C., Malm, O., Souza, C.M.M., Mierle, G., 1992. Mercury pollution in Brazil. *Nature* 356, 389. <https://doi.org/10.1038/356389a0>.
- Oliveira, S.M.B., Melfi, A.J., Fostier, A.H., Forti, M.C., Favaro, D.I.T., Boulet, R., 2001. Soils as an important sink for mercury in the Amazon. *Water Air Soil Pollut.* 26, 321–337. <https://doi.org/10.1007/s12665-018-7471-x>.
- Outridge, P.M., Sanei, H., Stern, G.A., Hamilton, P.B., Goodarzi, F., 2007. Evidence for control of mercury accumulation in sediments by variations of aquatic primary productivity in Canadian High Arctic lakes. *Environ. Sci. Technol.* 41, 5259–5265. <https://doi.org/10.1021/es070408x>.
- Padberg, S., 1990. *Mercury Determinations in Samples from Tapajós (Itaituba)*, vol. 13. Institut für angewandte Physikalische Chemie, Jülich, Germany.
- Paula Filho, Marins, R.V., Lacerda, L.D., 2015. Natural and anthropogenic emissions of N and P to the Paranaíba River Delta in NE Brazil. *Estuar. Coast. Shelf Sci.* 166 (A), 34–44. <https://doi.org/10.1016/j.ecss.2015.03.020>.
- Pfeiffer, W.C., Lacerda, L.D., Malm, O., Souza, C.M.M., Silveira, E.G., Bastos, W.R., 1989. Mercury concentrations in inland waters of gold mining areas in Rondonia, Brazil. *Sci. Total Environ.* (87/88), 233–240. [https://doi.org/10.1016/0048-9697\(89\)90238-6](https://doi.org/10.1016/0048-9697(89)90238-6).
- Power, M.J., Marlon, J., Ortiz, N., Bartlein, P.J., Harrison, S.P., Mayle, F.E., Ballouche, A., Bradshaw, R.H.W., Carcaillet, C., Cordova, C., et al., 2008. Changes in fire regimes since the last glacial maximum: an assessment based on a global synthesis and analysis of charcoal data. *Clim. Dyn.* 30, 887–907. <https://doi.org/10.1007/s00382-007-0334-x>.
- Prokoph, A., El Bilali, H., 2008. Cross-wavelet analysis: a tool for detection of relationships between paleoclimate proxy records. *Math. Geosci.* 40, 575–586. <https://doi.org/10.1007/s11004-008-9170-8>.
- Prospero, J.M., Glacum, R.A., Nees, R.T., 1981. Atmospheric transport of soil dust from Africa to South America. *Nature* 289 (5798), 570–572. <https://doi.org/10.1038/289570a0>.
- Rama-Corredor, O., Martrat, B., Grimalt, J.O., López Otaño, G.E., Flores, J.A., Sierro, F., 2015. Parallelisms between sea surface temperature changes in the western tropical Atlantic (Guiana Basin) and high latitude climate signals over

- the last 140 000 years. *Clim. Past* 11, 1297–1311. <https://doi.org/10.5194/cp-11-1297-2015>.
- Ramos, T.P.A., Ramos, R.T.C., Ramos, S.A.Q.A., 2014. Ichthyofauna of the Parnaíba River basin, northeastern Brazil. *Biota Neotropica* (14), 1–8. <https://doi.org/10.1590/S1676-06020140039>.
- Ratter, J.A., Ribeiro, J.F., Bridgewater, S., 1997. The Brazilian Cerrado vegetation and threats to its biodiversity. *Ann. Bot.* 80, 223–230. <http://doi.org/10.1006/anbo.1997.0469>.
- Richardson, P.L., Reverdin, G., 1987. Seasonal cycle of velocity in the Atlantic North Equatorial Countercurrent as measured by surface drifters, current meters, and ship drifts. *J. Geophys. Res.: Oceans* 92 (C4), 3691–3708. <http://doi.org/10.1029/JC092iC04p03691>.
- Richey, J.E., Hedges, J.I., Devol, A.H., Quay, P.D., Victoria, R., Martinelli, L., Bruce, R., 1990. Biogeochemistry of carbon in the Amazon River. *Limnol. Oceanogr.* 35, 352–371. <http://doi.org/10.4319/lo.1990.35.2.0352>.
- Rohling, E.J., Grant, K., Hemleben, C., Siddall, M., Hoogakker, B.A.A., Bolshaw, M., Kucera, M., 2007. High rates of sea-level rise during the last interglacial period. *Nat. Geosci.* 1 (1), 38–42. <https://doi.org/10.1038/ngeo.2007.28>.
- Rosa, R.S., Menezes, N.A., Britski, H.A., Costa, W.J.E.M., Groth, F., 2003. Diversidade, padrões de distribuição e conservação dos peixes da Caatinga. In: Leal, I.R., Tabarelli, M., Silva, J.M.C. (Eds.), *Ecologia e Conservação da Caatinga*. Editora Universitária da UFPE, Recife, pp. 135–162.
- Roulet, M., Lucotte, M., Saint-Aubin, A., Tran, S., Rhéault, I., Farell, N., De Jesus Da Silva, E., Dezencourt, J., Sousa Passos, C.J., Santos Soares, G., Guimaraes, J.R.D., Mergler, D., Amorim, M., 1998. The geochemistry of mercury in central Amazonian soils developed on the Alter-do-Chão formation of the lower Tapajós River Valley, Para state, Brazil. *Sci. Total Environ.* 223, 1–24.
- Roulet, M., Lucotte, M., 1995. Geochemistry of mercury in pristine and flooded ferrallitic soils of a tropical rain forest in French Guiana, South America. *Water Air Soil Pollut.* 80, 1079–1088.
- Roulet, M., Lucotte, M., Rheault, I., Tran, S., Farella, N., Canuel, R., Mergler, D., Amorim, M., 1996. Mercury in Amazonian soils: accumulation and release. In: *IV International Conference on the Geochemistry of the Earth's Surface*. International Association of Geochemistry and Cosmochemistry, Ilkley, Yorkshire, England, pp. 453–457.
- Ruth, U., Bigler, M., Röthlisberger, R., Siggaard-Andersen, M., Kipfstuhl, S., Goto-Azuma, K., Hansson, M.E., Johnsen, S.J., Lu, H., Steffensen, J.P., 2007. Ice core evidence for a very tight link between North Atlantic and east Asian glacial climate. *Geophys. Res. Lett.* 34, L03706. <https://doi.org/10.1029/2006GL027876>.
- Sachs, J.P., Anderson, R.F., 2005. Increased productivity in the subantarctic ocean during Heinrich events. *Nature* 434 (7037), 1118–1120. <http://doi.org/10.1038/nature03544>.
- Salmond, J.A., 2005. Wavelet analysis of intermittent turbulence in a very stable nocturnal boundary layer: implications for the vertical mixing of ozone. *Boundary-Layer Meteorol.* 114 (3), 463–488. <https://doi.org/10.1007/s10546-004-2422-3>.
- Santos, G.M., Cordeiro, R.C., Silva Filho, E.V., Turcq, B., Lacerda, L.D., Fifield, L.K., Gomes, P.R.S., Hausladen, P.A., Sifeddine, A., 2001. Chronology of atmospheric mercury in Lagoa da Pata Lake, upper Rio Negro region of Brazilian Amazon. *Radiocarbon* 43, 801–808. <http://doi.org/10.1017/S0033822200041473>.
- Schroeder, W.H., Munthe, J., 1998. Atmospheric mercury: an overview. *Atmos. Environ.* 32, 809–822. [https://doi.org/10.1016/S1352-2310\(97\)00293-8](https://doi.org/10.1016/S1352-2310(97)00293-8).
- Schulz, M., Mudelsee, M., 2002. REDFIT: estimating red-noise spectra directly from unevenly spaced paleoclimatic time series. *Comput. Geosci.* 28 (3), 421–426. [http://doi.org/10.1016/S0098-3004\(01\)00044-9](http://doi.org/10.1016/S0098-3004(01)00044-9).
- Schuster, E., 1991. The behavior of mercury in the soil with special emphasis on complexation and adsorption processes—A review of the literature. *Water Air Soil Pollut.* 56, 667–680. <https://doi.org/10.1007/BF00342308>.
- Selim, H.M. (Ed.), 2013. *Competitive Sorption and Transport of Heavy Metals in Soils and Geological Media*. CRC Press Taylor and Francis Group, p. 420pp.
- Sholupov, S., Pogarev, S., Ryzhov, V., Mashyanov, N., Stroganov, A., 2004. Zeeman atomic absorption spectrometer RA-915+ for direct determination of mercury in air and complex matrix samples. *Fuel Process. Technol.* 85, 473–485. In: <https://doi.org/10.1016/j.fuproc.2003.11.003>.
- Silveira, C.S., Brandão, V.S., Bernedo, A.V.B., Mantovano, J.L., 2016. Geochemistry of river suspended sediments in tropical watersheds: anthropogenic and granite-gneiss sources, SE Brazil. *Int. J. River Basin Manag.* 14 (4), 385–391. <https://doi.org/10.1080/15715124.2016.1213271>.
- Skonieczny, C., McGee, D., Winckler, G., Bory, A., Bradtmiller, L.L., Kinsley, C.W., Polissar, P.J., De Pol-Holz, R., Rossignol, L., Malaizé, B., 2019. Monsoon-driven Saharan dust variability over the past 240,000 years. *Sci. Adv.* 5 (1), eaav1887. <https://doi.org/10.1126/sciadv.aav1887>.
- Soerensen, A.L., Mason, R.P., Balcom, P.H., Jacob, D.J., Zhang, Y., Kuss, J., Sunderland, E.M., 2014. Elemental mercury concentrations and fluxes in the tropical atmosphere and ocean. *Environ. Sci. Technol.* 48, 11312–11319. <https://doi.org/10.1021/es503109p>.
- Stern, G.A., Sanei, H., Roach, P., Delaronde, J., Outridge, P.M., 2009. Historical interrelated variations of mercury and aquatic organic matter in lake sediment cores from a subarctic lake in Yukon, Canada: further evidence toward the algal-mercury scavenging hypothesis. *Environ. Sci. Technol.* 43, 7684–7690. <https://doi.org/10.1021/es902186c>.
- Steffen, A., Lehnerr, I., Cole, A., Ariya, P., Dastoor, A., Durnford, D., Kirk, J., Pilote, M., 2015. Atmospheric mercury in the Canadian Arctic. Part I: a review of recent field measurements. *Sci. Total Environ.* (509–510), 3–15. <https://doi.org/10.1016/j.scitotenv.2014.10.109>.
- Stouffer, R.J., Yin, J., Gregory, J.M., Kamenkovich, I.V., Sokolov, A., 2006. Investigating the causes of the response of the thermohaline circulation to past and future climate changes. *J. Clim.* 19 (8), 1365–1387. <https://doi.org/10.1175/JCLI3689.1>.
- Stramma, L., England, M., 1999. On the water masses and mean circulation of the South Atlantic Ocean. *J. Geophys. Res.* 104 (C9), 20863–20.
- Stramma, L., Fischer, J., Reppin, J., 1995. The North Brazil undercurrent. *Deep-Sea Res. Part I* 42 (5), 773–795. [http://doi.org/10.1016/0967-0637\(95\)00014-W](http://doi.org/10.1016/0967-0637(95)00014-W).
- Stríkis, N.M., Cruz, F.W., Barreto, E.A.S., Naughton, F., Vuille, M., Cheng, H., Sales, H.R., 2018. South American monsoon response to iceberg discharge in the North Atlantic. *Proc. Natl. Acad. Sci.* 115 (15), 3788–3793. <http://doi.org/10.1073/pnas.1717784115>.
- Svendsen, J.I., Alexanderson, H., Astakhov, V.I., Demidov, I., Dowdeswell, J.A., Funder, S., Gataullin, V., Henriksen, M., Hjort, C., Houmark-Nielsen, M., Hubberten, H.W., Ingolfsson, O., Jakobsson, M., Kjær, K.H., Larsen, E., Lokrantz, H., Lunkka, J.P., Lyså, A., Mangerud, J., Matiouchkov, A., Murray, A., Möller, P., Niessen, F., Nikolskaya, O., Polyak, L., Saarnisto, M., Siegert, C., Siegert, M.J., Spielhagen, R.F., Stein, R., 2004. Late Quaternary ice sheet history of northern Eurasia. *Quat. Sci. Rev.* 23, 1229–1271. <https://doi.org/10.1016/j.quascirev.2003.12.008>.
- Torrence, C., Webster, P.G., 1999. Interdecadal changes in the ENSO-monsoon system. *J. Clim.* 12, 2679–2690.
- Vandal, G.M., Fitzgerald, W.F., Boutron, C.F., Candelone, J.P., 1993. Variations in mercury deposition to Antarctica over the past 34,000 years. *Nature* 362 (6421), 621–623. <https://doi.org/10.1038/362621a0>.
- Venancio, I.M., Multiza, S., Govin, A., Santos, T.P., Lessa, D.O., Albuquerque, A.L.S., Chiessi, C.M., Tiedemann, R., Vahlenkamp, M., Bickert, T., Schulz, M., 2018. Millennial-to orbital-scale responses of western equatorial Atlantic thermocline depth to changes in the trade wind system since the Last Interglacial. *Paleoceanogr. Paleoclimatol.* 33. <https://doi.org/10.1029/2018PA003437>.
- Veres, D., Bazin, L., Landais, A., Toyé Mahamadou Kele, H., Lemieux-Dudon, B., Parrenin, F., et al., 2013. The Antarctic ice core chronology (AICC2012): an optimized multi-parameter and multi-site dating approach for the last 120 thousand years. *Clim. Past* 9 (4), 1733–1748. <https://doi.org/10.5194/cp-9-1733-2013>.
- Waelbroeck, C., Labeyrie, L., Michel, E., Duplessy, J.C., McManus, J.F., Lambeck, K., Labracherie, M., 2002. Sea-level and deep water temperature changes derived from benthic foraminifera isotopic records. *Quat. Sci. Rev.* 21 (1–3), 295–305. [https://doi.org/10.1016/S0277-3791\(01\)00101-9](https://doi.org/10.1016/S0277-3791(01)00101-9).
- Wang, X., Auler, A.S., Edwards, L.L., Cheng, H., Cristalli, P.S., Smart, P.L., Shen, C.C., 2004. Wet periods in northeastern Brazil over the past 210 kyr linked to distant climate anomalies. *Nature* 432 (7018), 740–743. <http://doi.org/10.1038/nature03067>.
- Wang, X., Auler, A.S., Edwards, R.L., Cheng, H., Ito, E., Solheid, M., 2006. Inter-hemispheric anti-phasing of rainfall during the last glacial period. *Quat. Sci. Rev.* 25 (23–24), 3391–3403. <https://doi.org/10.1016/j.quascirev.2006.02.009>.
- Wasserman, J.C., Hacon, S., Wasserman, M.A., 2003. Biogeochemistry of mercury in the Amazonian environment. *AMBIO A J. Hum. Environ.* 32 (5), 336–342. <https://doi.org/10.1579/0044-7447-32.5.336>.
- WHO, 1989. *Environmental Health Criteria 86: Mercury - Environmental Aspects (Geneva)*.
- Williams, R.H., McGee, D., Kinsley, C.W., Ridley, D.A., Hu, S., Fedorov, A., Tal, I., Murray, R.W., deMenoca, P.B., 2006. Glacial to Holocene changes in trans-Atlantic Saharan dust transport and dust-climate feedbacks. *Sci. Adv.* 2 (11), 1600445–1600445. <https://doi.org/10.1126/sciadv.1600445>.
- Zhang, Y., Chiessi, C.M., Multiza, S., Zabel, M., Trindade, R.I.F., Hollanda, M.H.B.M., Dantas, E.L., Govin, A., Tiedemann, R., Wefer, G., 2015. Origin of increased terrigenous supply to the NE south American continental margin during Heinrich stadial 1 and the younger Dryas. *Earth Planet. Sci. Lett.* 432, 493–500. <http://doi.org/10.1016/j.epsl.2015.09.054>.